The life cycle of human papillomavirus type 16 E6 variants and its effects on the innate immune system of host keratinocytes

A thesis presented to

The Faculty of Graduate Studies

of

Lakehead University

by

ROBERT JACKSON

In partial fulfillment of requirements
for the degree of
Master of Science in Biology

10 Sep 2012

ABSTRACT

Persistent infection with human papillomavirus type 16 (HPV16) is the primary aetiological agent for cervical cancer. Viral particles initiate their life cycle by infecting basal keratinocytes of epithelium and amplifying their genome. Viral oncoproteins E6 and E7 are responsible for causing host cells to proliferate, disrupting the regular differentiation regimen. Infections are typically cleared by a host immune response, but HPV16 is capable of persisting, increasing the chance of genomic integration and host cell transformation. It is thought that HPV16 can evade the innate immune response by down-regulating important molecules such as toll-like-receptors (TLRs): normally responsible for recognizing viral infection and activating immune-response genes by a signal transduction cascade. Epidemiological studies show natural E6 variants, Asian-American (AA) and L83V, are found more often than the prototype in invasive cervical cancers. Increased oncogenic potential for AA and L83V E6 genes has been confirmed by recent studies, but the role of the viral life cycle remains uncertain for each variant. The effects of an active viral life cycle on innate immunity were tested by first establishing an organotypic tissue culture model for mimicking HPV-infected epithelium. This model was phenotypically verified by morphology and immunohistochemistry for HPV16 L2 capsid protein, proliferation marker BrdU, and differentiation markers K5 and K10. Expression analysis for viral and innate immune genes was performed using RT-qPCR. Significantly, TLR3 and IFN-κ were down-regulated in AA and L83V variants compared to prototype HPV16, indicating a variant-specific viral life cycle effect on host innate immune defence. Future high-throughput analyses, such as microarray or RNA-sequencing, can be used for global expression profiling.

LAY SUMMARY

Faculty and students in the Department of Biology are bound together by a common interest in explaining the diversity of life, the fit between form and function, and the distribution and abundance of organisms. As we unravel the complexity of life we discover that disease occurs due to changes at the molecular level. The purpose of this research was to study the effect of human papillomavirus type 16 (HPV16), a cancer causing virus, on the natural immune defence of host cells. Previous studies show that genetic variations within the E6 gene of HPV16 are found more commonly in invasive cervical cancers. This fact raises the question: do these HPV16 E6 variants have an effect on our initial immune response, allowing infections to persist and lead to cancer? Since it is unethical to experiment on humans, it was necessary to establish life-like skin that can be grown in the lab to mimic the viral life cycle. My experiments verified that the life-like skin was able to support viral growth and that key genes responsible for an initial immune response are negatively affected. Not only does this research extend the frontier of biological knowledge, but it also has important implications for our understanding, diagnosis, treatment, and prognosis of cancers caused by human papillomavirus type 16.

DEDICATION

To those who undertake the methodical pursuit of truth.

ACKNOWLEDGEMENTS

Professional

First and foremost I would like to thank Dr. Ingeborg Zehbe for her key role as my mentor and thesis supervisor. Thank you to my committee members, and earlier mentors, Dr. Lada Malek and Dr. Wensheng Qin for seeding my interest in research during my undergraduate years and continuing the support to this day. Additionally, thank you goes to Dr. Lynne Hampson as my external examiner in the subject of viral oncology. Finally, thank you to Eleanor Maunula for all her administrative work and patience.

I must also express my gratitude to the Lakehead University professors that allowed me to assist with their courses: Dr. Lada Malek for Cell Biology, Dr. David Law and Dr. Chris Phenix for Biochemistry I lab, and finally, Dr. Greg Pyle for Biostatistics. Additionally, thank you to all the undergraduate and graduate students I had the pleasure of working with; I'm sure I learned more from you than you did from me.

Thank you to all past and present Thunder Bay Regional Research Institute (TBRRI) students, scientists, and employees. You all provided an atmosphere of constant learning and collaboration. Thank you to Dr. David Law and fellow grad student Mike Broere for the use of your lab for Experion analysis of RNA. Thank you David Nurse of the Thunder Bay Regional Health Sciences Centre for your histological processing and discussions. Thank you to Dr. Paul Lambert and Denis Lee for their technical assistance and providing NIKS. Thank you Dr. Martin Müller for providing anti-HPV16 L2 antibody.

Personal

Thankfully, I have the support of valued family, friends, comrades, and critters. I'm truly humbled by their collective intelligence, experience, compassion, and wit. I want to emphasize that these are the people that inspire me to push-on, and from which I build my character. Firstly, thank you to Miss Jessie Jones, for your loving support. You carried me, literally in some cases, through this time and for that I am truly grateful.

Thank you to my family, near and far, for your support throughout the years. I am forever appreciative of my father Arthur and mother Lina for their assistance and willingness to accept my life decisions. My younger sister Kate and brother Sterling, thanks for your understanding and time together. Thanks to Gram for her quick wit and unwavering support. Grazie Nono per l'ospitalità e esperienza di vita, però, mi dispiace informarvi che non sono ancora un dottore! Finally, thank you to Jackson cousin-brothers Ryan and Alex. Since childhood you've been pillars in my life; I don't see that ever changing.

I've been lucky enough to meet some exceptional people that I can fortunately say are friends. With over a decade of letting me be his sidekick, Mohammad Noroozi has been an amazing buddy. The biostats crew, consisting of Heidi Forsyth, Mike Broere, and Sarah Niccoli is another force to be reckoned with. Special thanks to Sarah, my lab-wife, for putting up with my pedantics (I think I just made up a word) and always being there to support me. NiccolJack sounds like a bad Canadian pop-rock group, but special extraordinary thanks for being my MSc war-buddy. Thanks to all the other students and lab members of TBRRI for the “out of the box” perspective and humour.

TABLE OF CONTENTS

LIST OF TABLES

LIST OF FIGURES

LIST OF ABBREVIATIONS

AA	Asian-American HPV16 E6 variant
bp	Base-pair
BrdU	Bromo-2-deoxyuridine
cDNA	Complementary DNA
CIN	Cervical Intraepithelial Neoplasia
CO_2	Carbon Dioxide
Ct	Cycle threshold
DAPI	4',6-diamidino-2-phenylindole
dH_2O	Distilled Water
DMEM	Dulbecco's Modified Eagle Medium
DMSO	Dimethyl Sulfoxide
DNA	Deoxyribonucleic Acid
dsDNA	Double Stranded Deoxyribonucleic Acid
DPBS	Dulbecco's Phosphate Buffered Saline
EBV	Epstein-Barr Virus
EDTA	Ethylenediaminetetraacetic Acid
EGF	Epidermal Growth Factor
FBS	Fetal Bovine Serum
FFPE	Formalin-Fixed, Paraffin-Embedded
GFP	Green Fluorescent Protein
HBV	Hepatitis B Virus
HPRT1	Hypoxanthine Phosphoribosyltransferase 1

HPV	Human Papillomavirus
ICC	Immunocytochemistry
IFN	Interferon
IHC	Immunohistochemistry
IL	Interleukin
LB	Lysogeny Broth
mAb	Monoclonal Antibody
mRNA	Messenger RNA
NIKS	Normal or Near-diploid Immortal Keratinocytes
p53	Tumour Suppressor Protein 53
PCR	Polymerase Chain Reaction
pRb	Retinoblastoma Protein
RNA	Ribonucleic Acid
RQI	RNA Quality Indicator
RT-qPCR	Reverse Transcription, Real-Time PCR
SOC	Super Optimal Broth with Catabolite Repression
TBE	Tris/Borate/EDTA
TLR	Toll-Like Receptor
UV	Ultraviolet

1 INTRODUCTION

1.1 Literature Review

1.1.1 Tumour Viruses

Although evidence for an infectious aetiology of cancers had been discovered throughout the 20th century, it was not until the 70's and 80's that the concept began to take hold within the medical and scientific community (Zur Hausen, 2007). The steady advance of biotechnology saw a shift toward a molecular basis for disease, and with that, the acceptance that infectious agents, such as viruses, can be carcinogenic. Overall, it's thought that greater than 20% of cancers worldwide are due to infections (Zur Hausen, 2007); prominent agents are Epstein-Barr virus (EBV), hepatitis B virus (HBV), and human papillomavirus (HPV). My thesis concerns the role of this last agent, HPV; subsequent pages review our understanding of its life cycle and carcinogenic abilities.

1.1.2 Normal Epithelium: Proliferation and Differentiation of Basal Keratinocytes

Human skin, or the integumentary system, is our first line of defence against the environment and infectious microorganisms (Miller and Harley, 2002). Skin consists of two main layers: epidermis and dermis. The dermis supports epidermal growth and contains fibroblasts, collagen fibre matrices, vessels, and glands. The epidermis consists of a stratified squamous epithelial layer: basal keratinocytes which proliferate and differentiate upward into flattened, keratinized cells at the surface (left-most part of **Figure 1**).

1.1.3 Human Papillomaviral Life Cycle

Human papillomaviruses (HPVs) are double-stranded DNA viruses that infect basal keratinocytes of skin and mucosa via micro-abrasions (zur Hausen, 2002). Infection with HPV is most common in the epithelia of the genital tract, resulting in benign ano-genital warts. However, with persistent infection, integration of the HPV genome into host genomic DNA can cause low-grade ano-genital lesions (such as cervical intra-epithelial neoplasia, CIN) progressing to invasive solid tumours of the cervix (**Figure 1**) (Woodman et al., 2007). HPVs are thus divided into two types based on their tumour-forming potential: low-risk and high-risk (Stanley et al., 2007). HPV type 16, which is also an aetiological agent for some head and neck cancers (Dayyani et al., 2010), is the most prevalent of the high-risk types and therefore an important subject for study (zur Hausen, 1996).

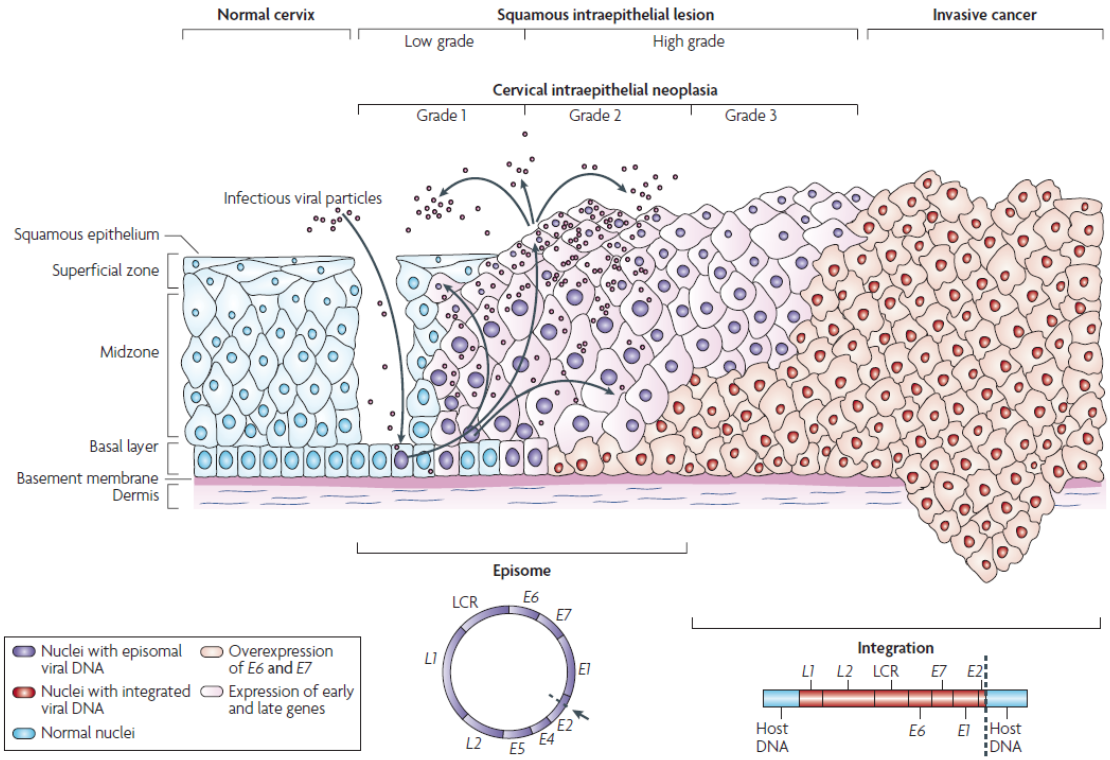

Figure 1. HPV-mediated progression to cervical cancer.

Viral particles infect basal keratinocytes through micro-abrasions. Expression of "early" viral genes allow episomal DNA replication. Following altered differentiation of keratinocytes, "late" expression enables viral DNA encapsidation and completion of the infectious viral life cycle. Infections may persist due to immune evasion causing genomic integration with potential progression to neoplasia or even invasive cancer (Woodman et al., 2007).

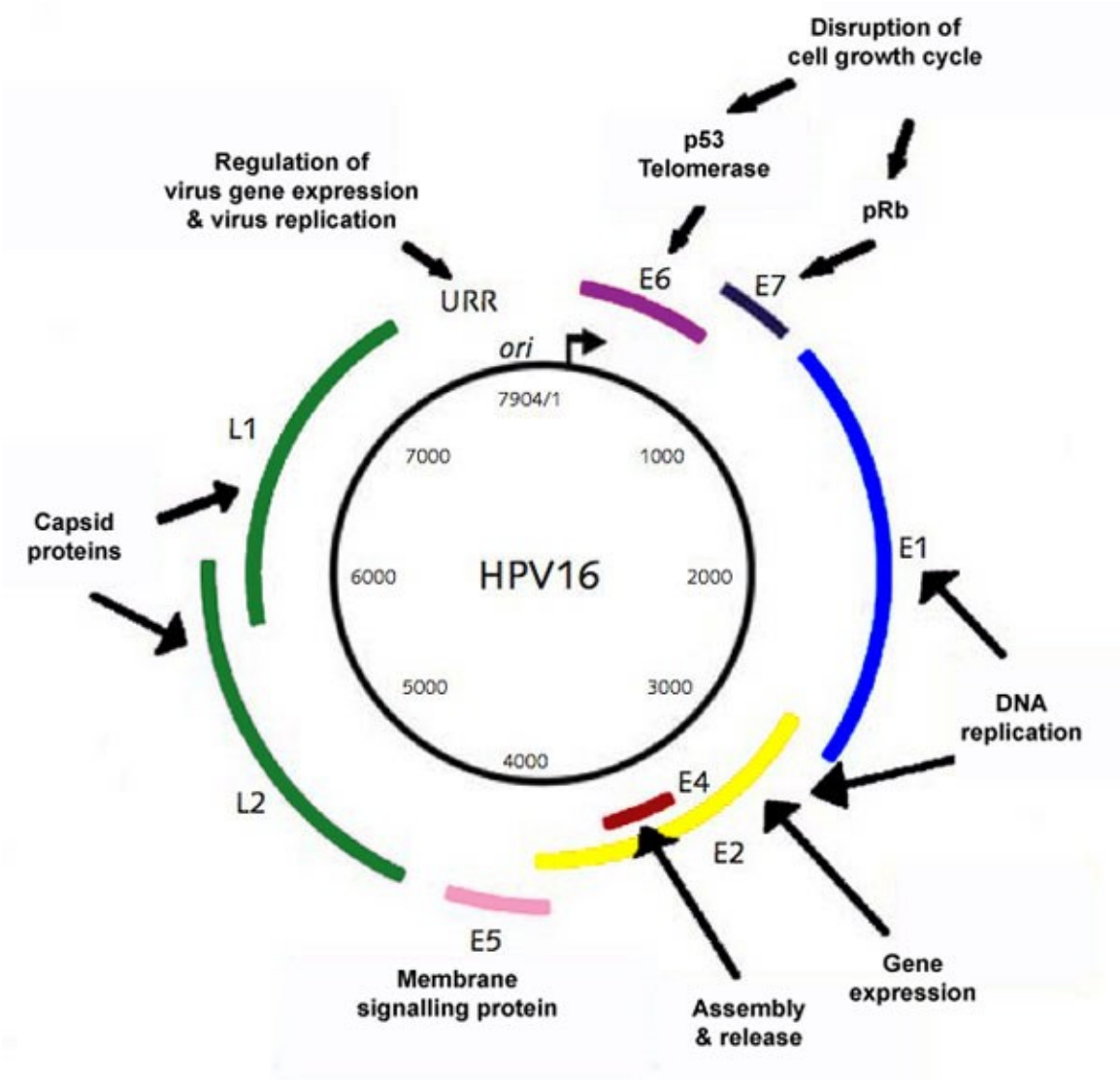

Figure 2. HPV16 genome and product roles.

Drawing of the 8 kb HPV16 genome showing the regulatory region for viral gene expression, the eight genes, and the roles of each protein product (Cann, 2007).

The complete HPV16 genome (**Figure 2**) is approximately 8 kb long and consists of a long control region (LCR/URR) for transcription of eight genes (six early expressed and two late expressed). The human papillomaviral life cycle begins when virus gains entry to basal keratinocytes followed by uncoating its protective capsid proteins (Doorbar, 2005). The viral genome is maintained episomally at a low-copy number, replicating along with the host DNA, aided by the E1 and possibly E2 proteins. Rather than following normal differentiation, infected cells continue to proliferate into the suprabasal layers due to E6 and E7 protein products disrupting cell cycle progression (Hamid et al., 2009): E6 disrupts tumour suppressor protein 53 (p53) and E7 disrupts retinoblastoma protein (pRb). Once in the upper layers of epithelium, the late promoter, residing in the E7 open reading frame, leads to an increase in E1, E2, E4, and E5, and ultimately viral genome amplification (Doorbar, 2005). A third late-gene product, the spliced transcript E1^E4, is present during early expression, but most abundant during the productive stage of a viral life cycle (Bodily et al., 2011). E1^E4 has been used as a marker for initiation of viral transcription and quantitatively as a measure of viral life cycle productivity. Once the viral genome has been amplified in the upper layers, E4 aids viral capsid synthesis with the activation of L1 and L2 proteins, encapsulating the viral DNA. Viral life cycle is completed when infectious virus is released back into the environment.

In cases of persistent host cell infection, viral DNA can integrate into the host genome, causing an interruption of the E2 gene (Stanley et al., 2007). Loss of E2 leads to uncontrolled expression of E6 and E7, eventually leading to uncontrolled proliferation and immortalization of host cells (**Figure 1**). The transformation mechanism of HPV16

E6 was unravelled following the discovery of its numerous cellular binding partners. The two zinc-binding domains and C-terminal PDZ-binding domain allow interaction with a variety of cellular proteins, with many that act at a transcriptional level (Mantovani and Banks, 2001; Kumar et al., 2002). Along with E6-associated protein (E6AP), HPV16 E6 binds to and causes ubiquitinlyation and eventual proteosomal degradation of tumour suppressor protein p53 *in vitro* and *in vivo* (Lechner et al., 1992; Scheffner et al., 1992; Lagrange et al., 2005). Disruption of p53-mediated cellular response to DNA damage, which normally initiate the intrinsic apoptotic regimen of a cell, has also been demonstrated with E6 (Kessis et al., 1993).

1.1.4 The Innate Immune System

The innate immune system, also called the nonspecific defence system, is responsible for first-line protection and raising the alarm (Wilson et al., 2011). Skin, as a physical barrier of differentiated keratinocytes, is the initial defence against invasion by microorganisms. However, when this barrier is breached, internal mechanisms of defense must be able to recognize pathogens and initiate an immune response. Trans-membrane receptor proteins, such as toll-like receptors (TLRs), are able to recognize foreign molecules and initiate a signal transduction cascade leading to immune-response gene expression (Wilson et al., 2011) (**Figure 3**). Viral recognition by TLRs results in downstream activation of important signalling molecules: interferons (IFNs) and inflammatory cytokines (Stanley et al., 2007). These are important for protecting the infected and surrounding cells as well as amplifying the immune response. Interestingly, there has been increasing evidence of a link between HPV immune evasion and oncogenicity (O'Brien and Campo, 2003).

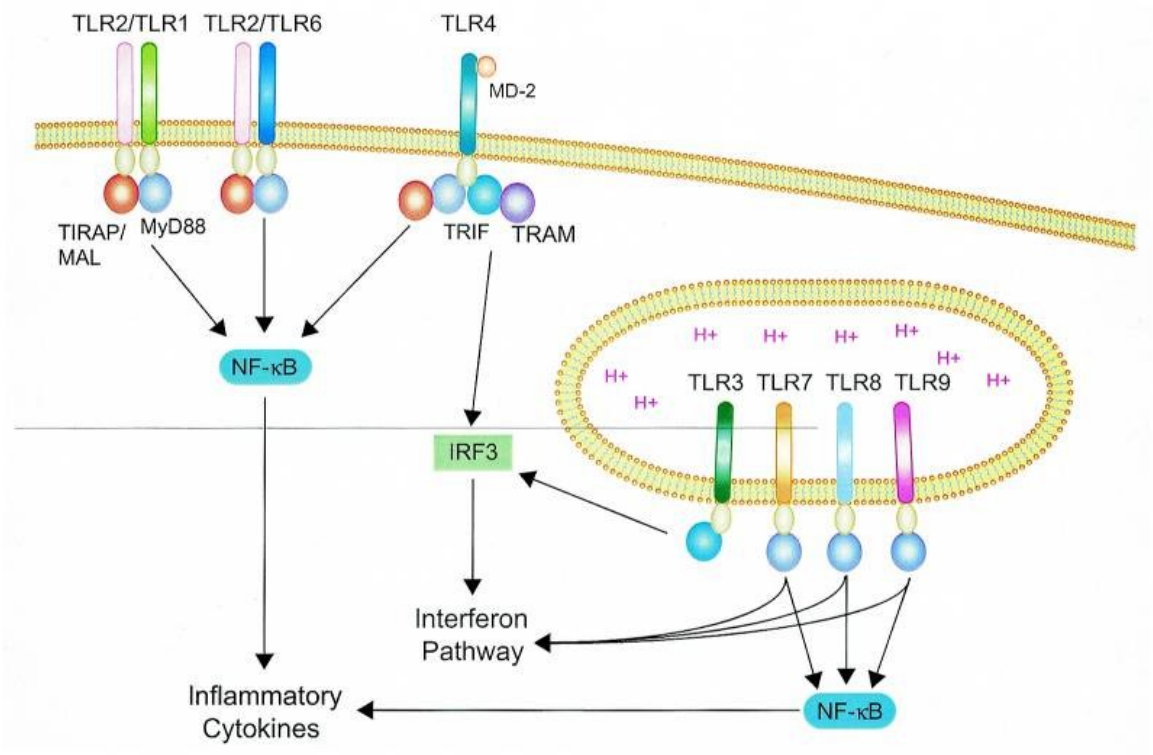

Figure 3. Antiviral innate immune response.

TLRs 1, 2, 4, and 6 can identify extracellular molecules and initiate a signal transduction cascade to activate inflammatory cytokines. TLRs 3, 7, 8, and 9 span endosomal membranes and can identify foreign molecules within cells, such as nucleic acids, initiating interferon and inflammatory cytokine activation (Boehme and Compton, 2004).

1.1.5 Infectomics

Broad gene expression changes, including those beyond the repression and induction of inflammatory molecules, can be studied using bioinformatics. This application of information technology to molecular biology, allows for system-wide analysis and understanding of biological systems. By obtaining global expression profiles of samples (via Affymetrix microarray or recently, RNA-sequencing) it's possible to identify patterns and networks of molecular interactions that are representative of an experimental manipulation. Infectomics is the systems biology study of infected host tissue; in other words, an infectome represents all the host molecular changes in response to a pathogen (Navratil et al., 2011).

1.2 Research Rationale

Epidemiological studies have uncovered naturally-occurring HPV16 E6 polymorphisms leading to variations in the amino acid sequence of the E6 oncoprotein (Zehbe et al., 1998). These variants are described based on their geographic distribution and origin of discovery: European prototype (first described), L83V, and Asian-American (AA, Q14H/H78Y/L83V). Amino acid sequence variations are identified in **Figure 4**. Most interestingly, these epidemiological studies indicate variant-specific prevalences in invasive cervical cancer due to suspected higher oncogenic potential of AA and L83V compared to prototype. Research has already been undertaken to determine the role of HPV16 E6 variants on oncogenic potential, mimicking a persistently infected and post-integrated scenario (Zehbe et al., 2009). They differ in their ability to alter keratinocyte differentiation and p53 degradation (Stoppler, 1996). Additionally, recent studies on

primary human foreskin keratinocytes demonstrate *in vitro* transformation and increased migratory abilities by AA E6 alone (Richard et al., 2010; Niccoli et al., 2012). However, there is a significant knowledge gap; the full-length variant genomes have not been studied for initial effects in an early infection scenario. Taken with the fact that the majority of HPV infections are normally cleared, there is justification to consider that increased prevalence of HPV16 E6 variants in malignant tumours may be due to unique or augmented viral life cycle effects early-on within host cells. Given that HPV16 is known to evade viral recognition and response by modulating interferon and toll-like receptors (Stanley et al., 2007), the innate immune system is a good place to start looking for variant-specific effects before conducting costly high-throughput analyses.

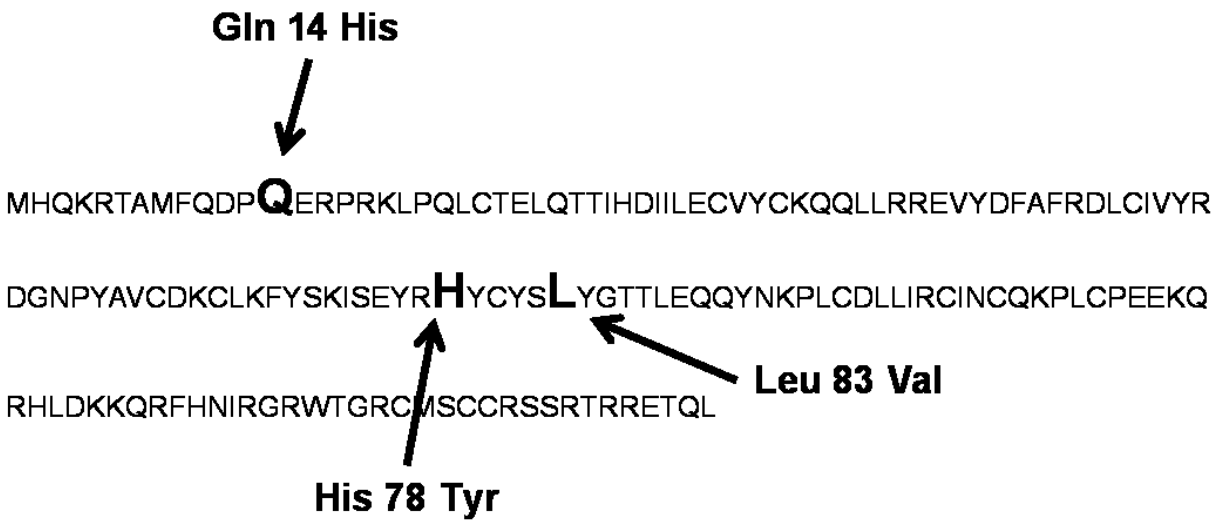

Figure 4. Naturally occurring E6 oncoprotein variations.

The amino acid sequence of prototype HPV16 E6 oncoprotein is 151 residues long from N-terminus to C-terminus. E6 has many cellular binding partners due to its two zinc-binding domains. The L83V variant has a valine (Val, V) in place of a leucine (Leu, L) at the 83rd residue. The Asian-American variant (AA) has the L83V change in addition to a histidine (His, H) replacing glutamine (Gln, Q) at residue 14 and tyrosine (Tyr, Y) replacing histidine (His, H) at residue 78.

1.3 Hypotheses

Given epidemiological and laboratory findings, it's hypothesized the Asian-American (AA) HPV16 E6 variant will be most successful in viral proliferation and host immune evasion. The null hypotheses are that there will be no differences in viral proliferation and host evasion between the variants.

1.4 Research Aims

1. Establish an organotypic raft infrastructure to facilitate the coincidence of HPV16 E6 variant life cycles with keratinocyte differentiation.
2. Phenotypically characterize the organotypic cultures by morphological and immunohistochemical assessment.
3. During the active viral life cycle, study molecular relationships of the innate immune system in the context of the variants; verify the model system for future high-throughput analyses.

1.5 Method Development

As famously paraphrased from statistician George E. P. Box, "all models are wrong, but some are useful" (Box, 1976; Box et al., 1976). Although Box referred primarily to mathematical models, the concept can also be applied to experimental models. Manipulative experiments require a relevant model system for valid inferences, and in the case of this project, one that is capable of normal skin growth (differentiation regimen) and supporting an active viral life cycle. A review of human epidermis modelling highlights the history, variety, and use of organotypic tissues for research (Poumay and Coquette, 2007).

Within the HPV research community, two prominent organotypic tissue culture doctrines have emerged: Lambertian and Meyersian. The Lambert lab developed a reliable culturing technique using normal immortalized keratinocytes (NIKS) capable of harbouring episomal viral copies and undergoing a full differentiation regimen (Flores et al., 1999; Flores et al., 2000; Genther et al., 2003; Lambert et al., 2005). To introduce full-length viral DNA into NIKS a chemical co-transfection strategy was employed in these studies. Meyers group, however, typically used a one-plasmid strategy with electroporation to introduce viral DNA (Yasumoto et al., 1986; McCance et al., 1988; Meyers et al., 2002). Due to established contacts and material availability the development of the model system employed herein was primarily influenced by Lambert lab methods. However, model optimization was required to establish a reliable procedure in our lab.

2 MATERIALS AND METHODS

2.1 Cell Culture

2.1.1 Cell Lines and Routine Maintenance

Human cell cultures were maintained in a 37°C humidified incubator supplemented with 5% carbon dioxide (CO_2) gas. Nutrient growth media was replaced every second day and cells were passaged (sub-cultured) at approximately 70% confluence. Sterile Dulbecco's phosphate buffered saline (DPBS; Invitrogen, Cat. No. 14190) was used to remove any residual medium prior to cell detachment via trypsinization. Aseptic technique was strictly followed to maintain sterility and prevent

contamination. Cells were negative for *Mycoplasma* contamination as indicated by routine testing.

Normal or near-diploid immortalized keratinocytes (NIKS), which are capable of a normal differentiation regimen and can maintain the HPV genome episomally, were grown on mitomycin-C-treated Swiss mouse J2/3T3 fibroblast feeder layers (Allen-Hoffmann et al., 2000). Confluent J2/3T3 fibroblast cells, maintained normally in Dulbecco's Modified Eagle Medium (DMEM; Sigma-Aldrich, Cat. No. D5796) supplemented with 10% fetal bovine serum (FBS; Sigma-Aldrich, Cat. No. F6178) and 1% antibiotic/antimycotic (Invitrogen, Cat. No. 15240-062), were reproductively inactivated by a two hour treatment with 4 μg/mL of mitomycin-C (Roche Canada, Cat. No. 107409). Inactivated feeders were sub-cultured at 10-20% density and incubated at least two hours and up to 48 hours before adding keratinocytes. NIKS were maintained in keratinocyte culture medium made up of 3 parts Ham's F-12 medium (Invitrogen, Cat. No. 21700-075) supplemented with 7.5% sodium bicarbonate (Invitrogen, Cat. No. 25080-094), 1 part DMEM (Sigma-Aldrich, Cat. No. D5796), 2.5% FBS (Sigma-Aldrich, Cat. No. F6178), 0.4 μg/mL hydrocortisone (Sigma-Aldrich, Cat. No. H4001), 8.4 ng/mL cholera toxin (Sigma-Aldrich, Cat. No. C8052), 5 μg/mL insulin (Sigma-Aldrich, Cat. No. I5500), 24 μg/mL adenine (Sigma-Aldrich, Cat. No. A2786), and 10 ng/mL epidermal growth factor (EGF; R&D Systems, Cat. No. 236-EG). NIKS were passaged between 1:5 and 1:10 with incomplete NIKS medium (without EGF) for the first 24 hours to allow stable growth, followed by a change to complete medium every other day for routine growth. When splitting NIKS, feeder cells were first removed by a short incubation with trypsin-ethylenediaminetetraacetic acid (trypsin-EDTA; Invitrogen, Cat.

No. 25300062) followed by vigrous washing with DPBS (Invitrogen, Cat. No. 14190). Feeder fibroblasts are less adherent and can be removed this way without disturbing the strongly adherent keratinocytes. NIKS transfected with full-length HPV16 DNA from three different E6 variants (prototype, L83V, and AA) were used as experimental treatments. NIKS containing the full-length episomal HPV16 genome (L83V variant, gift from Paul Lambert) were used as a positive control while untransfected NIKS were used as a negative control.

Primary human foreskin fibroblasts (ATCC CRL-2097) used for the dermal equivalent of organotypic raft cultures were only used at early-passage and maintained in human fibroblast medium: Ham's F-12 medium (Invitrogen, Cat. No. 21700-075) or DMEM, supplemented with 10% FBS (Sigma-Aldrich, Cat. No. F6178) and 1% antibiotic/antimycotic (Invitrogen, Cat. No. 15240-062).

Cervical carcinoma cell lines SiHa, CaSki, and C33A were all maintained in DMEM (Sigma-Aldrich, Cat. No. D5796) supplemented with 10% FBS (Sigma-Aldrich, Cat. No. F6178) and 1% antibiotic/antimycotic (Invitrogen, Cat. No. 15240-062). SiHa (ATCC HTB-35), which contains several integrated HPV16 copies per cell, was used as a positive control (Friedl et al., 1970). CaSki (ATCC CRL-1550), which contains about 600 copies per cell of integrated HPV16 and some HPV16 sequences, was also used as a positive control (Pattillo et al., 1977). C33A (ATCC HTB-31), which is a HPV negative cervical carcinoma cell line, was used as a negative control (Auersperg, 1964).

2.1.2 Cryogenic Storage of Cells

Confluent cells were prepared for cryogenic storage by aspirating growth medium followed by washing with sterile DPBS (Invitrogen, Cat. No. 14190) to remove any

residual medium. Cells were then lifted from the growth flask by incubating with trypsin-EDTA (Invitrogen, Cat. No. 25300062) for 5 minutes at 37°C with 5% CO_2. After confirming cells were lifted using an inverted microscope the trypsin-EDTA was inactivated by adding 9 parts growth medium. Total number of cells was determined by sampling 10 µL with a TC10™ Automated Cell Counter (Bio-Rad, Cat. No. 145-0009) or 200 µL with a Coulter Particle Counter (Beckman Coulter Canada, Mississauga, ON). Unless otherwise desired, 1 x 10^6 cells were centrifuged at 25 x g (Beckman GS-6KR Centrifuge) for five minutes, re-suspended in 900 µL of growth medium, and added to 1.5 mL cryovials (Thermo Fisher Scientific, Cat. No. 66008-710) with 100 µL of the cryoprotectant dimethyl sulfoxide (DMSO; Sigma-Aldrich, Cat. No. 34869): 1 mL aliquots of 90% growth medium and 10% DMSO. Labelling conventions, *e.g.* "NIKS P3 RJ 28 Dec 2010", were consistently applied: cell identity, passage number, user, and date. Cryovials were placed in a controlled-rate cooling container (Thermo Fisher Scientific, Cat. No. 5100-0001), cooled to -80°C at 1°C/min, and subsequently transferred to liquid nitrogen for long-term cryogenic storage (Nunc Nalgene, 1998).

2.1.3 Thawing Cells

Cryovials were safely removed from liquid nitrogen storage and immediately thawed to room temperature. Adhering to aseptic technique, the cryovial contents (1 mL) were transferred into a 15 mL conical tube containing 9 mL of the appropriate growth medium. Cryoprotectant (DMSO) was removed by centrifugation at 25 x g (Beckman GS-6KR Centrifuge) for 5 minutes followed by aspiration of the supernatant. The cell pellet was re-suspended in growth medium, seeded into an appropriately sized growth vessel, and incubated at 37°C with 5% CO_2 for normal growth. Alternatively, the thawed

cryovial contents were seeded directly into growth medium and vessel, effectively diluting the DMSO to non-toxic levels. Medium was changed the next day to ensure removal of any residual DMSO.

2.1.4 Mycoplasma Testing and Treatment

Mycoplasma are a genus of prokaryotes that lack a cell wall, conferring resistance to common antibiotics, that are an insidious contaminant of mammalian cell culture. Contaminations can persist and cause metabolic stress, arginine depletion (Schimke et al., 1966), poor transfection efficiencies (Xia et al., 1997), and gene expression changes (Jung et al., 2003) to host cultures; *Mycoplasma* can be quite problematic for experimental studies (Russell et al., 1975; Chen, 1977).

Due to the risk of contamination effects on experiments, cells were tested regularly for *Mycoplasma* contamination by fluorescent 4',6-diamidino-2-phenylindole (DAPI) staining. A strict regimen was established to track and limit the spread of *Mycoplasma*. Aseptic technique, along with thorough surface sterilization with 70% ethanol and ultraviolet (UV) radiation, was employed as a front-line defence. Furthermore, separation of culturing time, location, and reagents were maintained when handling potentially contaminated cultures (or those with unknown *Mycoplasma* history). All work with these "quarantine" cultures was delayed until after routine culturing to limit cross-contamination. Separate incubators and bio-safety cabinets were also used. As an additional precaution, reagents necessary for the maintenance of "quarantine" cultures were aliquoted for single-use to prevent contamination of working solutions.

Cultures were tested initially upon arrival, prior to making freeze-backs, and at least once a month during routine growth. Cells were grown at least one week in culture

after being established from cryogenic storage to allow detectable titres of contaminants to develop. Enough cells were seeded onto a sterilized glass cover slip (Thermo Fisher Scientific, Cat. No. 12-541A), placed in a 35 mm culture dish (VWR, Cat. No. CA25382-064) by sterile forceps, to yield at least 50% confluency after 2-3 days. At which point, medium was removed from sub-confluent cells and replaced with a modified Carnoy's fixative (3 parts methanol (Thermo Fisher Scientific, Cat. No. A4544) to 1 part glacial acetic acid (Sigma-Aldrich, Cat. No. 695092-2.5L)) for 5 minutes. Fixative was removed and replaced with fresh fixative for an additional 10 minutes. Fixative was then removed and cover slips were allowed to air dry. The cover slips were mounted to a microscope slide using Vectashield mounting medium with DAPI (1.5 µg/mL, Vector Laboratories, Cat. No. H-1200) and allowed at least 5 minutes in the dark prior to fluorescent detection. Mounted slides were stored at 4°C in the dark if necessary. A fluorescence microscope with an excitation filter for 360 nm was used to visualize a 460 nm emission of blue-fluorescing DNA. *Mycoplasma* were identified at 400X or 1000X (oil-immersion) magnification as small cocci or rods within or outside of a cell, distinct from cell nuclei (**Figure 5**).

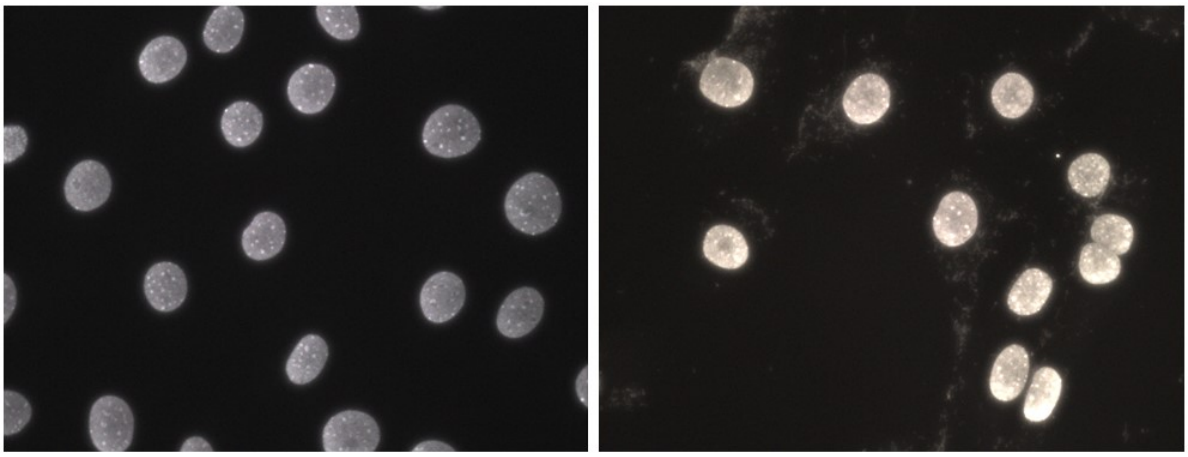

Figure 5. J2/3T3 fibroblast nuclei stained with DAPI at 400X magnification.

Adherent cells were cultured on cover glass in a 35 mm dish. Sub-confluent cells were fixed in Carnoy's fixative (3 parts methanol to 1 part glacial acetic acid), stained with DAPI, and mounted to a microscope slide. The 400X magnified image was captured using a Zeiss fluorescence microscope with 100 ms exposure for excitation/blue emission at 358/461 nm. The right image shows intracellular *Mycoplasma* contamination.

The preferred response to *Mycoplasma* contamination was immediate bleach disinfection and disposal of the culture. When this was not possible, such as with precious cell lines, treatment was attempted. BM Cyclin (Roche Canada, Cat. No. 10799050001), a set of drugs targeting bacterial ribosomal protein synthesis was used to treat *Mycoplasma* infected cultures (Fleckenstein and Drexler, 1996). Cells were treated for three weeks while alternating between BM Cyclin I and II, and grown for a final week in the absence of BM Cyclin before being screened.

2.2 Establishment of Recombinant Viral Variant Constructs

Recombinant DNA constructs of full-length HPV16 E6 variants were previously created by site-directed mutagenesis (Flores et al., 1999) and verified by DNA sequencing. Full-length viral DNA for each HPV16 E6 variant (Prototype, L83V, and AA) was cloned into the multiple cloning site of the high-copy number pUC19 (**Figure 6**).

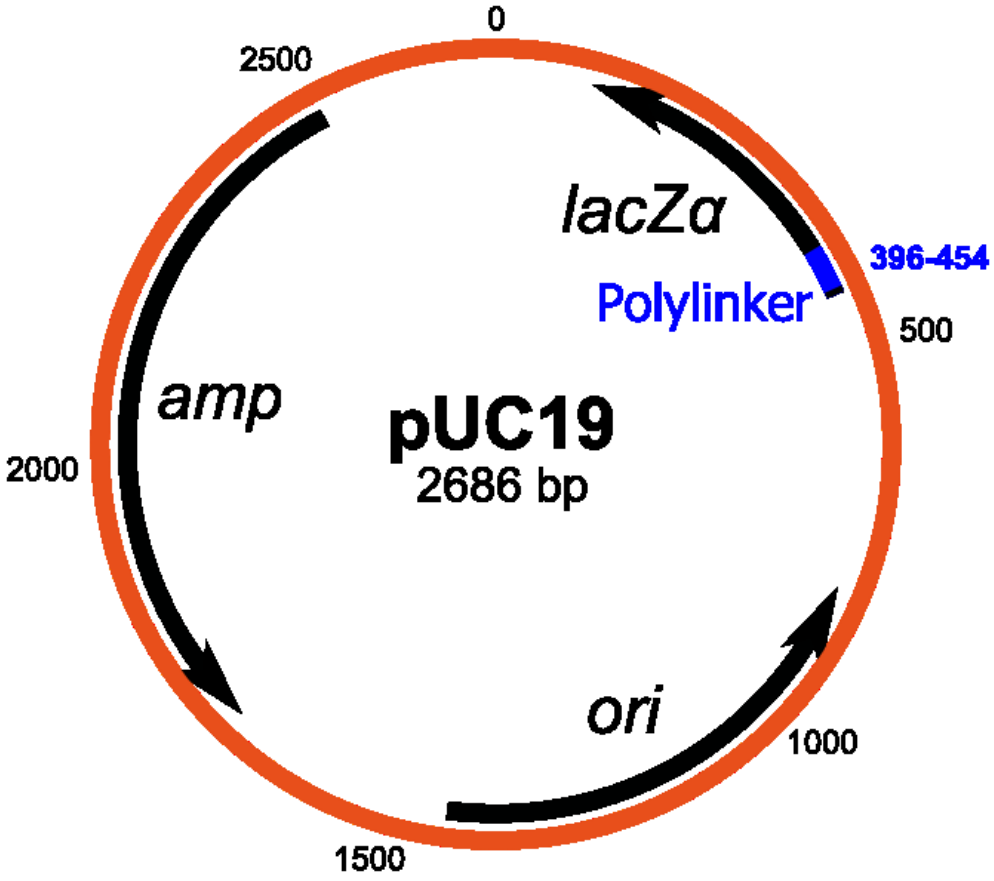

Figure 6. Vector map of the 2686 base-pair (bp) empty pUC19 plasmid cloning vector (public domain).

2.3 Viral DNA Isolation and Preparation

2.3.1 Handling, Storage, Quantification, Purity, and Integrity of DNA

DNA was handled cautiously to avoid mechanical damage such as genomic shearing or plasmid nicking; vigorous pipetting and vortexing was explicitly avoided. DNA was stored in appropriate buffers (*e.g.*, TRIS) and kept at 4°C for general short-term storage. Plasmid DNA was kept at -20°C for long-term storage. Double-stranded DNA (dsDNA) samples were quantified using a Take3 micro-volume plate with a Synergy 4 spectrophotometer (BioTek, Winooski, VT). Sample volumes of 1 to 2 µL were measured and blanked with corresponding storage buffer. Absorbance was measured at wavelengths of 260 and 280 nm, yielding final concentration (ng/µL) and purity ($A_{260/280}$). Pure nucleic acid samples, with low levels of detectable protein impurities, were indicated by $A_{260/280} \geq 1.8$. Integrity of DNA was verified by agarose gel electrophoresis. Intact DNA had a discrete band of the appropriate size.

2.3.2 Bacterial Transformation and Purification of Plasmid DNA

Plasmid cloning vectors were transformed into competent *E. coli* cells followed by kit-based plasmid purification. Viral constructs, containing full-length viral DNA within the multiple cloning site of the high-copy number pUC19 (**Figure 6**), conferred ampicillin resistance as a selective marker. Another type of ampicillin resistance-conferring plasmid, pReceiver-MO3 (**Figure 7**), was used for its coding of green fluorescent protein (GFP) and neomycin resistance.

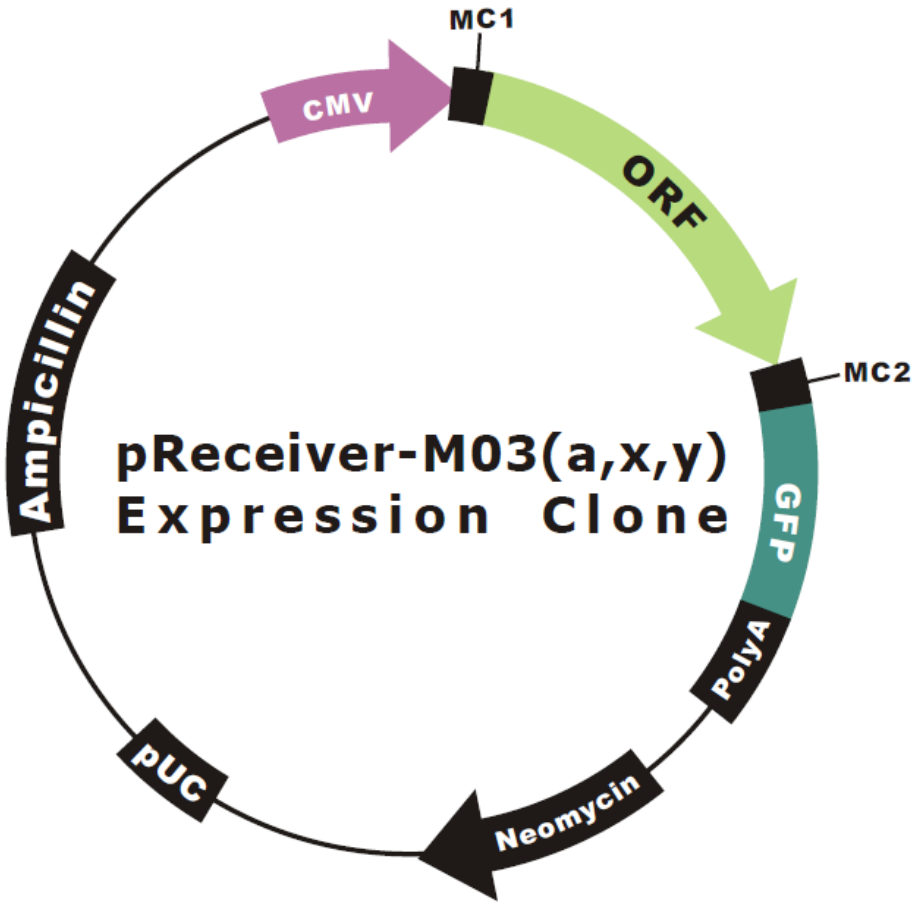

Figure 7. Vector map of pReceiver-M03 plasmid cloning vector (GeneCopoeia).

First, selective agar plates were made by combining and stirring one LB (lysogeny broth) agar tablet (Sigma-Aldrich, Cat. No. L7025-500TAB) per 50 mL of distilled water (dH_2O) in a 500 mL Erlenmeyer flask for two minutes. The flask was covered with aluminum foil and autoclaved on the liquid cycle to fully dissolve the tablets and sterilize the resulting solution. A 54°C water bath was used to cool the sterilized solution prior to the aseptic addition of ampicillin (Sigma-Aldrich, Cat. No. A9518-5G, stock 50 mg/mL) to a final concentration of 100 µg/mL. The LB agar plates were poured and allowed to dry in the tissue culture bio-safety cabinet. Extra plates were stored upside-down in a bag or saran wrap at 4°C.

Next, one vial of 5-alpha competent *E. coli* cells (New England BioLabs, Cat. No. C2992H), stored at -80°C, was thawed on ice for 10 minutes for each construct needed. At least 1 µL of desired plasmid DNA was added to the bacterial cell mixture followed by gentle mixing. The mixture was then placed on ice for 30 minutes, heat shocked in a 42°C water bath for 30 seconds, and placed on ice for another 5 minutes. A volume of 950 µL room temperature super optimal broth with catabolite repression (SOC, New England BioLabs) medium was added followed by 60 minutes of 37°C shaking at 250 rpm (Barnstead International, Max^{Q} ™ Mini 4450). Whilst shaking, selective agar plates made previously were warmed to 37°C in the bacterial incubator. After shaking, cells were mixed thoroughly by flicking and inversion. Selective agar plates were spread with 75 µL each and incubated overnight at 37°C in the bacterial incubator.

Broth was prepared as agar before, but rather with LB broth tablets (Sigma-Aldrich, Cat. No. L7275-500TAB). The sterile solution was stored at room temperature and flame sterilized before and after each use. Aliquots of 5 mL LB broth in 15 mL

conical tubes were supplemented with 100 µg/mL of ampicillin. A single colony from each construct's plate was chosen, scooped using a sterile pipette tip, and placed into the 5 mL of LB broth. Plates with remaining colonies were stored at 4°C and could be used for up to one month. Conical tube lids were slightly loosened before shaking at 37°C and 300 rpm for 8 hours.

After the 8 hour growth and for each construct, 500 µL of cell suspension was added to 250 mL of LB broth with 100 µg/mL of ampicillin in a 1 L flask. These were covered with aluminum foil and placed in the shaker at 37°C and 300 rpm overnight. Additional 8 hour growth suspension was used to make glycerol stocks: 0.8 mL of cell suspension was added to 0.2 mL of 80% sterile glycerol (USB, Cat. No. US16374) in a cryovial (Thermo Fisher Scientific, Cat. No. 03-337-7Y). Glycerol stocks were stored at -80°C. When needed, a portion of frozen glycerol stock was scraped off and streaked onto an ampicillin-selective LB agar plate using a flame sterilized metal inoculating loop. The glycerol stock was returned to -80°C prior to thawing to prevent bacterial death. The streaked selective plate was incubated at 37°C overnight, followed by repetition of the same protocol.

After the final overnight growth, the cell suspension was aliquoted into 50 mL conical tubes (40 mL per tube). These were centrifuged at 6000 x g (Beckman Coulter Allegra™ 25R Centrifuge) for 15 minutes, followed by removal of supernatant by decanting, and purification of plasmid DNA using Qiagen's EndoFree Plasmid Maxi Kit (Qiagen, Cat. No. 12362). Bacterial cell pellets were stored at -20°C if not proceeding directly with purification.

2.3.3 Restriction Enzyme Digestion

Viral DNA was isolated from the pUC19 vector by first using a restriction endonuclease reaction. A total of 10 µg of each variant's plasmid DNA was digested in four separate reactions (2.5 µg of DNA each) for 3 hours at 37°C using 10 U of buffered BamH1 enzyme (Thermo Fisher Scientific, Cat. No. ER0055). Reagents were combined in a microcentrifuge tube and made up to a 20 µL volume with nuclease-free water, incubated at 37°C for 3 hours, briefly centrifuged to prevent sample loss, and finally combined into a single tube of 80 µL per variant. Digested samples, containing the full-length viral DNA and the linearized cut plasmid, were stored at 4°C if not proceeding directly with purification or -20°C for long-term storage.

2.3.4 Agarose Gel Electrophoresis and Purification of DNA

Full-length viral DNA was isolated from the remaining plasmid DNA by gel electrophoresis followed by purification. A 0.8% agarose gel (PCR certified agarose; Bio-Rad, Cat. No. 161-3104) in Tris/Borate/EDTA (TBE) buffer including 0.5 µg/mL ethidium bromide (Invitrogen, Cat. No. 15585-011) was cast using a horizontal mini-gel apparatus and allowed to polymerize for 45 minutes with a 100 µL well-comb. Loading dye (6X, Fermentas, Cat. No. R0611) was added to restriction digested samples, 5 µL of GeneRuler™ 1 kb (Fermentas, Cat. No. SM0314) was used as a DNA ladder, while samples were split and loaded into two lanes to prevent spill over. Electrophoresis was run at 100 V for 2 hours to allow sufficient separation between empty plasmid DNA and full-length linearized HPV DNA.

Once the run was complete, a UV imager (BioSpectrum 410 Imaging System, UVP) was used with 365 nm transillumination and 0.1 seconds exposure to capture

images. The viral DNA was isolated from empty plasmid by excising the DNA bands from the agarose gel with a clean scalpel and use of a UV transillumination table. DNA pieces were cut out quickly to avoid UV damage and transferred to pre-weighed microcentrifuge tubes. Microcentrifuge tubes were re-weighed and gel purification was performed using Qiagen's QIAquick Gel Purification Kit (Qiagen, Cat. No. 28704). Each piece of agarose with DNA was purified and eluted with 30 µL. Purified DNA was quantified and tested for quality before proceeding to ligation.

2.3.5 Ligation of Purified Viral DNA

Purified viral DNA was re-circularized as a full-length uninterrupted genome by performing ligation reactions. Each 20 µL ligation reaction was performed in a 0.2 mL tube with 1 µg of purified viral DNA, 2 µL T4 DNA ligase buffer (10X; Cedarlane, Cat. No. M0202S), and 1 µL of T4 DNA ligase enzyme (Cedarlane, Cat. No. M0202S). Nuclease-free dH_2O was used if necessary to make up the reaction volume to 20 µL. Ligations were performed overnight at 16°C in a thermocycler (2720 Thermal Cycler, Applied Biosystems). Final prepared variant DNA was either used immediately for transfection or stored at 4°C.

2.4 Transfection of Viral DNA into an Immortalized Cell Line

2.4.1 Preparation of Immortalized Keratinocytes

NIKS were cultured as described earlier, trypsinized, and counted; 2.4 x 10^6 cells total were required for duplicate transfections of 4 x 10^5 cells/12.5 cm^2 flask (VWR, Cat. No. CA29185-298). These cells were seeded out 24 hours prior to transfection. NIKS were seeded without feeders to increase transfection efficiency, but had to be maintained with low calcium NIKS medium and no EGF to prevent calcium-induced differentiation.

2.4.2 Co-transfection Strategy

Since the re-ligated full-length HPV16 variant genomes contain no selective marker a co-transfection strategy was employed. The full-length genomes were transfected into NIKS with an equal amount of plasmid containing genes for GFP and neomycin (G418) resistance. Under these conditions it is theoretically possible that four general cell populations would exist: NIKS with neither plasmid, NIKS with HPV16 but no GFP/neo plasmid, NIKS with GFP/neo but no HPV16, and NIKS with HPV16 and GFP/neo plasmid. Under selective conditions, we would expect about half of the remaining population to have HPV16 DNA.

FuGENE 6 Transfection Reagent (Roche Applied Science, Cat. No. 11814443001) was used 3:1 to DNA (6 µL FuGENE reagent to 1 µg each of HPV16 and plasmid DNA). Cells were first washed with PBS and media was replaced with low calcium NIKS complete medium. The transfection reagent was incubated in 94 µL serum-free Ham's F12 for 5 minutes followed by 15 minutes with the DNA after flicking to mix. The transfection solution was added drop-wise and flasks were moved back and forth to evenly distribute the delivery. Cells were incubated at 37°C and 5% CO_2 for 24 hours. After 24 hours, transfected NIKS were split onto reproductively inactive feeder layers with regular NIKS incomplete medium (without EGF). These were incubated another 24 hours prior to selection.

2.4.3 G418 Selection

To isolate colonies of successfully transfected NIKS, geneticin sulphate G418 (neomycin; VWR, Cat. No. CA12001-688) was used as a selective agent over the course of 5 days. Day 1 of selection, beginning 48 hours after transfection and 24 hours after a

new feeder layer, saw the addition of 100 µg/mL of G418. On the second day fresh feeders were added to replace those killed by selection. Day 3 saw media changed with the addition of 50 µg/mL of G418. Feeders were again replaced on the fourth day. Day 5 was the end of selection and media was not supplemented with G418 any longer. Fresh feeders were added again on day 6, followed by normal culturing of the cells.

2.5 Characterization and Verification of Transfection Efficiency

2.5.1 GFP Transfection Efficiency

Cells were observed under a fluorescent microscope 24 and 48 hours after transfection to verify transfection efficiency. For quantification of efficiency, 5 random fields of view were imaged in phase-contrast and fluorescence. The number of fluorescent cells in each was compared to the total number of cells, yielding percent transfection efficiency. However, given that GFP expression may be low and non-visible this indirect verification method was superseded by PCR detection of viral DNA.

2.5.2 Presence of Viral DNA

DNA was extracted from early passage transfectants using the DNeasy Blood & Tissue Kit (Qiagen, Cat. No. 69504). Cells were harvested from culture as described previously, with a pellet of 5 x 10^5 cells frozen and stored at -80°C until extraction. Kit instructions were followed, with duplicate 100 µL elutions performed for each sample. Extracted DNA was quantified as previously described.

Presence of viral DNA was assessed using DNA polymerase chain reaction (PCR) for HPV16 E6. PCR reactions were made up to 25 µL with nuclease-free dH_2O and the following master mix components: 1X PCR Buffer, 1 mM $MgCl_2$, 200 µM dNTPs, 0.5 µM forward E6 primer (5'-CAATGTTTCAGGACCCACA-3'), 0.5 µM reverse E6 primer

(5'-GTTTCTCTACGTGTTCTTGA-3'), 2 U Taq Polymerase, and 100 ng template DNA. No-template controls were run with each reaction. Thermocycler (2720 Thermal Cycler, Applied Biosystems) parameters were as follows: 40 cycles of 1 min 94°C denaturation, 1 min 60°C annealing, and 2 min 72°C extension. Final extension was performed for 7 min at 72°C followed by a 4°C hold. Gel electrophoresis was performed as described previously to visualize the expected 448 bp amplicon. PCR products were loaded onto a 1.5% agarose gel along with a 100 bp DNA ladder (New England BioLabs, Cat. No. N0467), and run for 1 hr at 100 V.

2.6 Establishment of Organotypic "3D Raft" Cultures

2.6.1 Preparation of the Dermal Equivalent

Early-passage human foreskin fibroblasts, cultured as described earlier, were trypsinized and counted; 1 x 10^6 cells were resuspended in 2 mL of FBS (enough for 1 x 10^5 cells/dermal equivalent). A sterilized small glass beaker and magnetic stir-rod, contained on ice, atop a magnetic stirring plate, were used to mix the following components for 8-10 equivalents whilst avoiding bubbles: 7.5 mL undiluted rat tail collagen type I (3.75 – 4.00 mg/mL; Millipore, Cat. No. 08-115), 1 mL Hanks' Balanced Salt solution (10X, Modified, without calcium, magnesium or sodium bicarbonate; Sigma-Aldrich, Cat. No. H4385), 30 µL of 5 *N* sodium hydroxide to neutralize the collagen and initiate gel solidification, and 2 mL of thoroughly resuspended fibroblasts (1 x 10^6 cells). The stirring speed was slightly increased and 1 mL of dermal equivalent mix was quickly and carefully pipetted into each of 8-10 wells in a 24 well plate. Some loss was expected due to excess bubbles and viscosity. Dermal equivalents were incubated for 20 minutes at 37°C and 5% CO_2 to allow solidification (verified by opaque appearance

and inversion test). This process was repeated as necessary depending on the required number of cultures; typically, three preparations were performed consecutively to yield a minimum of 24 dermal equivalents. Finally, 1 mL of fibroblast growth medium was added to each dermal equivalent well followed by overnight incubation at 37°C and 5% CO_2. Next day, homogenous distribution and elongation of fibroblasts was confirmed before proceeding.

2.6.2 Addition of Keratinocytes

Normal immortalized keratinocytes (NIKS), cultured as described earlier, were trypsinized and counted; 3 x 10^6 cells were thoroughly resuspended in 1 mL NIKS complete medium (enough for 6 rafts; 5 x 10^5/raft). Fibroblast medium was carefully removed from the dermal equivalents and 100 µL of keratinocytes were added to each well. After evenly distributing the cells across the dermal equivalent the keratinocytes were allowed to attach for 2 hours at 37°C and 5% CO_2. This process was repeated for each NIKS variant. Following this incubation period 1 mL of NIKS complete medium was added to each well. Rafts were once again incubated overnight at 37°C and 5% CO_2. Next day, homogenously distributed and 100% confluent keratinocytes were confirmed before proceeding.

2.6.3 Lifting Rafts for Stratification

NIKS medium was carefully removed from the rafts without puncturing the gel. Prior to lifting the rafts to the air-liquid interface, sterile cell culture inserts (30 mm, hydrophilic PTFE membrane, 0.4 µm; Millipore, Cat. No. PICM0RG50) were inserted into 6-well plates along with the addition of 1.1 mL of FAD medium (NIKS medium without EGF and with 1.88 mM Ca^{2+}) to the bottom. Rafts were then lifted onto the

membranes using a Pasteur pipette to loosen and a sterilized scoop to transfer the gels. Any fluid that formed on top of the membrane was removed so that the cells may only be fed through the bottom of the membrane. To allow epithelial stratification and viral life cycle , rafts were incubated at 37°C and 5% CO_2 for 14 days, changing media every second day. For a batch of 6 rafts, half were randomly designated for histological processing and half for RNA extraction. On day 14, rafts destined for histology were supplemented with 1.1 mL FAD medium containing 10 μM of thymidine analog bromo-2-deoxyuridine (BrdU) for 24 hours.

2.7 Phenotypic Characterization of Rafts

2.7.1 Histological/Morphological Assessment of Harvested Rafts

Half the rafts were harvested on day 15 for histological analysis by first washing away any residual media with PBS. Rafts were fixed by submersion in 10% formalin for 24 hours at room temperature. After formalin-fixation the rafts were washed and submerged in 70% ethanol. The histology lab of the Thunder Bay Regional Health Sciences Centre processed the tissue by bisecting, embedding in paraffin wax, sectioning by microtome (4 μm thickness), and mounting on positively-charged microscope slides. One pair of sections from each raft was haematoxylin and eosin stained for visualization of histological features. The remaining sections were provided unstained.

2.7.2 Immunohistochemistry: Viral Life Cycle, Proliferation, and Differentiation

Phenotypic characterization included confirming presence and localization of HPV16 L2 capsid protein for active viral life cycle, BrdU for proliferation, and K5/K10 for differentiation. Formalin-fixed, paraffin-embedded (FFPE) tissue slides were prepared by oven-baking at 60°C for 1 hour or alternatively, 37°C overnight. Paraffin was

removed by a series of triplicate 100% xylenes (Fisher Scientific, Cat. No. X3S-4) washes followed by triplicate 100% ethanol washes. Antigen retrieval was performed with 0.01 M citrate buffer and a pressure cooker (Pascal, Dako Cytomation) at 125°C and 20 psi. Monoclonal mouse primary antibodies for HPV16 L2 (Gift from Dr. Martin Müller, #4D11), BrdU (Invitrogen, Cat. No. ZBU30), and K10 (DAKO, Cat. No. M7002) were diluted 1:100 in background reducing diluent (Dako, Cat. No. S3022) and applied overnight at 4°C in a dark humidified chamber. Double-staining for K5 (together with K10) was done with rabbit polyclonal antibody K5 (Abcam, Cat. No. ab24647-50) diluted 1:10,000. As a negative technical control, diluent was used. Unbound primary antibody was removed by triplicate 10 min PBS washes. For HPV16 L2, BrdU, and K10, donkey anti-mouse secondary antibody-conjugated to Alexa Fluor® 594 (1:800, Life Technologies, Cat. No. A-21203) was applied for 30 min at room temperature in a dark humidified chamber. For K5, donkey anti-rabbit secondary antibody-conjugated to Alexa Fluor® 488 (1:400, Life Technologies, Cat. No. A-21206) was used. Unbound secondary antibody was removed by triplicate 10 min PBS washes followed by triplicate dH_2O washes. Slides were mounted using Vectashield with DAPI (1.5 µg/mL, Vector Laboratories, Cat. No. H-1200) and stored in a light-protected slide organizer.

Fluorescence was visualized and digitally captured using an inverted fluorescent microscope (Zeiss Axiovert 200 with mbq 52 ac power supply), digital camera attachment (QImaging QICAM Q21310), and Northern Eclipse software. For 350 nm emission (blue), 100 ms exposure time was used. For 488 nm (green) and 594 nm (red), 2.5 or 5.0 s exposure time was used. Images were captured with 1x1 binning, 1280x1024 resolution, 2.26% gain, 50.01% offset, and saved as ".bmp". Post-capture modifications

(such as overlays) were performed using ImageJ (version 1.47a, Schneider et al., 2012) and applied consistently to all image sets. Background fluorescence was subtracted by digital thresholding followed by linear adjustments to brightness and contrast.

2.8 RNA Expression Profiling

2.8.1 Handling and Storage of RNA

All RNA samples were stored at -80°C and only handled after using RNase-removing sprays on gloved hands and work surfaces. Sterile nuclease-free dH_2O was used for dilutions, nuclease-free plasticware, filter tips, and independent micropipettors were used for all pipetting.

2.8.2 RNA Extraction

Half the rafts were harvested for RNA extraction by first washing away residual medium with PBS. Sterile forceps were used to detach the epithelium and dermis into separate pre-labelled sterile nuclease-free 2 mL cryovials. Harvested samples were immediately flash-frozen using liquid nitrogen and stored at -80°C. RNA was extracted using the Arcturus PicoPure RNA Isolation Kit (Applied Biosystems, Cat. No. KIT0204), with the optional DNase treatment, and eluted in 30 µL of provided elution buffer.

2.8.3 Quantification, Integrity, and Purity Assessment of RNA

RNA quantity (in ng/µL) and integrity (28S:18S) was assessed using the Bio-Rad Experion Automated Electrophoresis system with a StdSens Analysis microfluidics kit (Bio-Rad, Cat. No. 700-7111). RNA quality indicator (RQI) values above 7.0 were considered representative of non-degraded RNA. A Take3 micro-volume plate with a Synergy 4 spectrophotometer (BioTek, Winooski, VT) was used to assess RNA purity

($A_{260/280}$). Pure nucleic acid samples, with low levels of detectable protein impurities, were indicated by $A_{260/280} \geq 1.9$. RNA samples were diluted to 100 ng/µL.

2.8.4 Reverse Transcription of RNA to cDNA

Prior to Reverse Transcription Real-Time PCR (RT-qPCR), RNA was reverse transcribed to complementary DNA (cDNA) using the High Capacity cDNA Archive Kit (Applied Biosystems, Cat. No. 4322171). Reactions were made up to 60 µL with the following master mix components: 1X RT buffer, 1X primers, 1X dNTPs, multiscribe enzyme, nuclease-free dH_2O, and 30 µL RNA template. No-template controls were run with each reaction. Thermocycler (2720 Thermal Cycler, Applied Biosystems) parameters were as follows: 10 min 25°C, 120 min 37°C, and 5 min 85°C followed by a 4°C hold.

2.8.5 Relative Expression by Real-Time Polymerase Chain Reaction

Viral mRNA transcript expression, along with others of interest, was analyzed by RT-qPCR with the Applied Biosystems 7500 Real-Time PCR System. Reactions consisted of 150 ng of cDNA, 45 µL of TaqMan® Gene Expression Master Mix (Applied Biosystems, Cat. No. 4369016), 4.5 µL of TaqMan® Gene Expression Assay hydrolysis probes (**Table 1**), and nuclease-free dH_2O to make up volume to 90 µL. Triplicate reaction volumes of 25 µL were loaded into a transparent 96-well plate and analyzed. To assess inter-plate variability, a positive tumour control along with negative control of nuclease-free dH_2O was run on each plate with the reference gene hypoxanthine phosphoribosyltransferase 1 (HPRT1). HPRT1 was chosen as a suitable reference gene based on previous optimization experiments (DeCarlo et al., 2008).

Table 1. Gene expression assays used for RT-qPCR (Applied Biosystems).

TaqMan® Gene Expression Assay	Assay ID
HPRT1	Hs99999909_m1
*HPV16 E6	AIAAY0O
*HPV16 E7	AIBJW6W
*HPV16 E1^E4	AIT9552
TLR3	Hs00152933_m1
TLR4	Hs00152937_m1
TLR7	Hs00152971_m1
TLR8	Hs00152972_m1
TLR9	Hs00152973_m1
IFN-β	Hs00277188_s1
IFN-γ	Hs00174143_m1
IFN-κ	Hs00737883_m1
IFN-λ (IL-29)	Hs00601677_g1

* denotes custom-designed assay

2.8.6 Data Analyses and Statistics

Cycle threshold (Ct) data was exported as comma-separated value (".csv") files, and organized for analysis in Microsoft Office Excel 2007. For viral gene expression, since the control sample has zero expression, relative expression was calculated by the modified Livak method ($2^{(Ct(ref) - Ct(target))}$). For non-viral gene expression, where the use of a calibrator sample was possible, relative expression ratio was calculated by the Livak

method ($2^{-\Delta\Delta Ct}$, Livak and Schmittgen, 2001). Both methods assume amplification efficiencies of the reference and target gene similarly close to 100%: $E = 2$.

All statistical analysis and subsequent figure creation was performed using the statistical programming language R (version 2.15.0; R Development Core Team, 2010). Significance level (α) was set, *a priori,* at 0.05. Data was determined to meet parametric assumptions based on normality, homogeneity of variance, and independence. Normality was tested using histogram, Q-Q plots, and Shapiro-Wilk's test. Homogeneity of variance was tested using a Bartlett or Levene test. If parametric assumptions were met, an ANOVA was employed with Tukey's HSD post-hoc if appropriate. Non-parametric data was either transformed to reclaim parametric assumptions, or subjected to the non-parametric Kruskal-Wallis test followed by Nemenyi or pair-wise Wilcoxon rank-sum post-hoc. Unless otherwise indicated, data are presented as means +/- SEM.

3 RESULTS

3.1 Establishment of Full-Length HPV16-Containing Keratinocytes

3.1.1 Isolation of HPV16 DNA from Restriction Digested Plasmid

Restriction endonuclease BamHI was successfully used to cut the full-length HPV16 genomes from their 2.7 kb plasmids (**Figure 8**). All three E6 variants had similar yield of viral DNA.

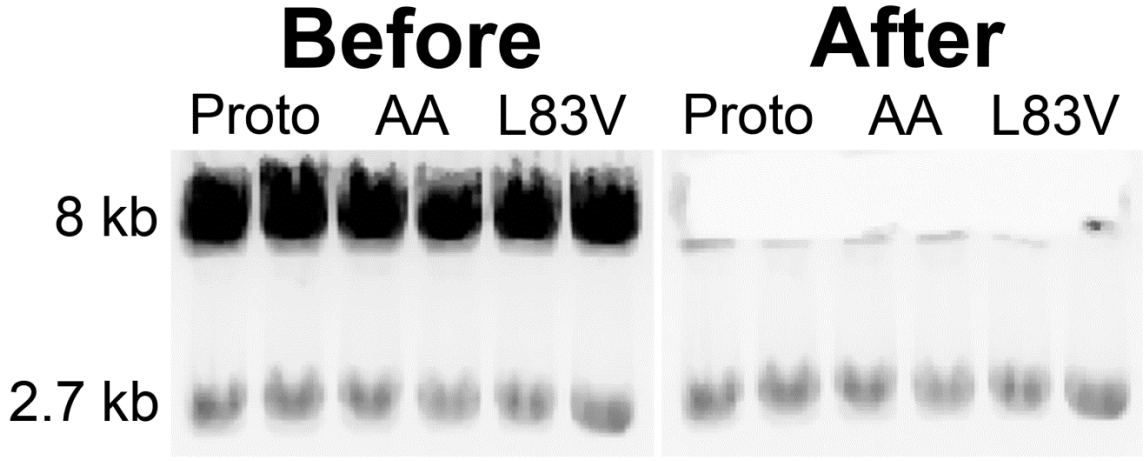

Figure 8. Gel electrophoresis of BamHI digested plasmid DNA.

A 0.8% agarose gel was used to separate restriction digested HPV DNA from its vector. Before and after gel excision of 8 kb-sized viral genome is shown; the remaining pUC19 plasmid at 2.7 kb is seen below. Lanes 1-2: Prototype; Lanes 3-4: AA; Lanes 5-6: L83V.

3.1.2 GFP Transfection Efficiency

Fluorescent detection of GFP positive cells was an indirect and poor indicator of transfection success. Typically, after 24 and 48 hours, 10-30% of cells were GFP positive. However, GFP expression dropped off and was not evident during or after selection. A more reliable transfection validation technique was used.

3.1.3 Presence of HPV16 E6 DNA

DNA PCR for HPV16 E6 was performed for direct evidence of transfection success (**Figure 9**). All three HPV16 E6 variants that were co-transfected had E6 amplicons of expected size and similar intensity. Untransfected NIKS was used as a negative control.

3.2 Development of Organotypic Tissue Culture Model

3.2.1 Elongation of dermal fibroblasts

A major checkpoint in the development of organotypic tissue cultures was verification of the dermal equivalents. Rafts were checked 24 hours after preparing the collagen matrix with embedded dermal fibroblasts for two key characteristics: homogenous distribution of fibroblasts throughout the dermis and elongation. Rafts were only continued if these criteria were met **(Figure 10**).

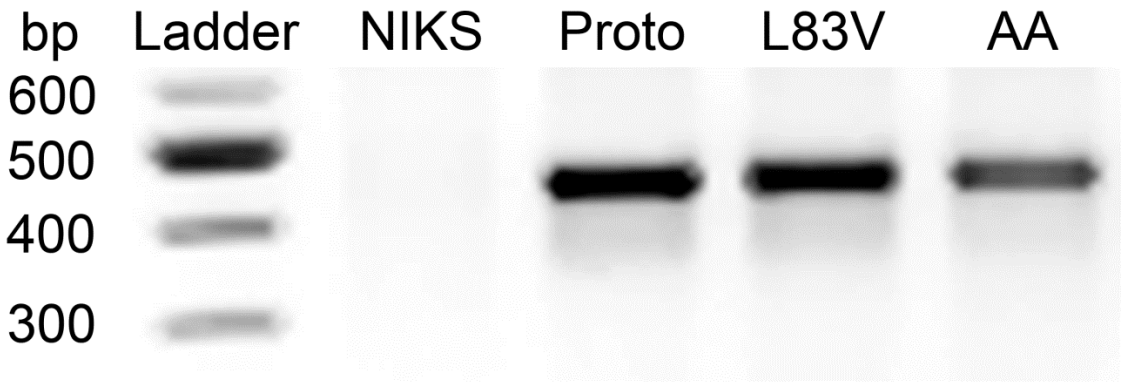

Figure 9. Gel electrophoresis of HPV16 E6 DNA PCR products.

A 1.5% agarose gel was used to assess E6 PCR products (448 bp amplicon). Lane 1: 100 bp DNA ladder; Lane 2: NIKS only; Lanes 3-5: NIKS16+ Proto, L83V, and AA.

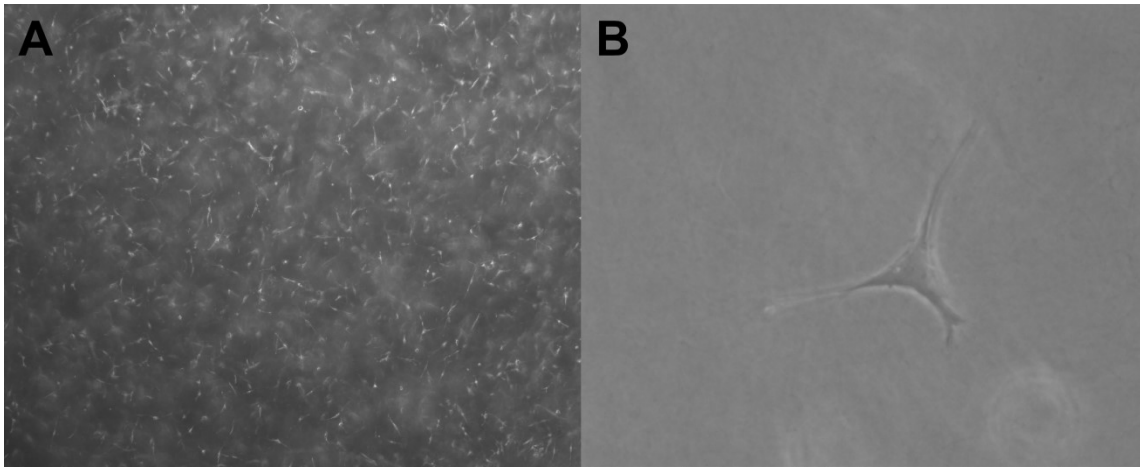

Figure 10. Fibroblasts in dermal equivalent after 24 hours.

Phase-contrast images of homogenously distributed and elongated fibroblasts embedded within the dermal equivalent of organotypic tissue culture: (A) 25X magnification shows homogenous distribution and (B) 400X magnification shows elongation of individual fibroblast.

3.3 Phenotypic Characterization of Organotypic Tissue Culture

3.3.1 General Morphology

Rafts had fully differentiated epithelium on the distal perimeter of each circular culture (**Figure 11**). The medial areas were thinner in comparison (only a monolayer of cells in some cases). Overall, untransfected NIKS epithelium appeared to be the thinnest while the three variants had thicker layers. In some cases there are obvious squamous/keratinized cells (corresponding to stratum granulosum and perhaps lucidum) in uppermost layers. In prototype and L83V cultures, some keratinized areas were seen in middle layers.

3.3.2 Evidence of an Active Viral Life Cycle: HPV16 L2 Capsid Protein IHC

HPV16 L2 capsid protein was used as a marker for the viral life cycle, observed in the upper layers. L2 staining was seen in all variant replicates, in upper layers, but not consistently across entire sections (**Figure 12**). No specific L2 staining was seen in untransfected NIKS. There appeared to be less capsid protein in AA compared to Proto and L83V. The squamous layer of some sections separated, likely due to processing.

3.3.3 Proliferation Marker: BrdU IHC

BrdU was added to culture medium 24 hours before harvesting. HPV16-containing rafts are known to have suprabasal proliferation and therefore would contain BrdU-positive suprabasal cells (Flores et al., 1999). In untransfected NIKS, only basal cells had BrdU incorporation (**Figure 13**). In Proto and L83V there was some suprabasal incorporation. In AA almost all suprabasal cells had some BrdU incorporation.

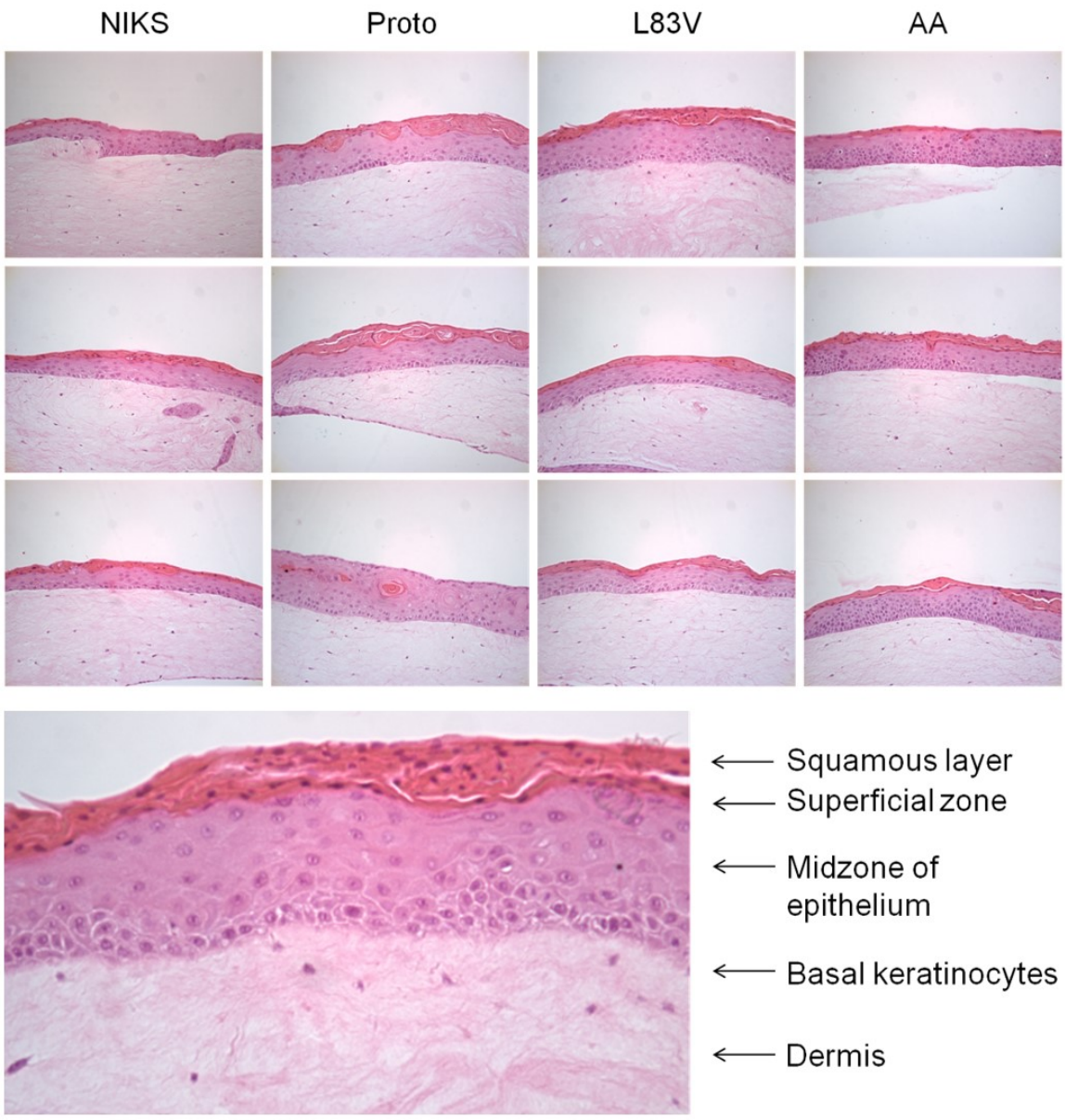

Figure 11. General morphology of raft cultures.

Haematoxylin and eosin stain of sectioned formalin-fixed paraffin-embedded raft cultures (200X magnification, biological triplicates). A differentiated epidermal layer is seen above the dermal equivalent collagen with fibroblasts. Below, the skin layers are labelled in an enlarged representative image.

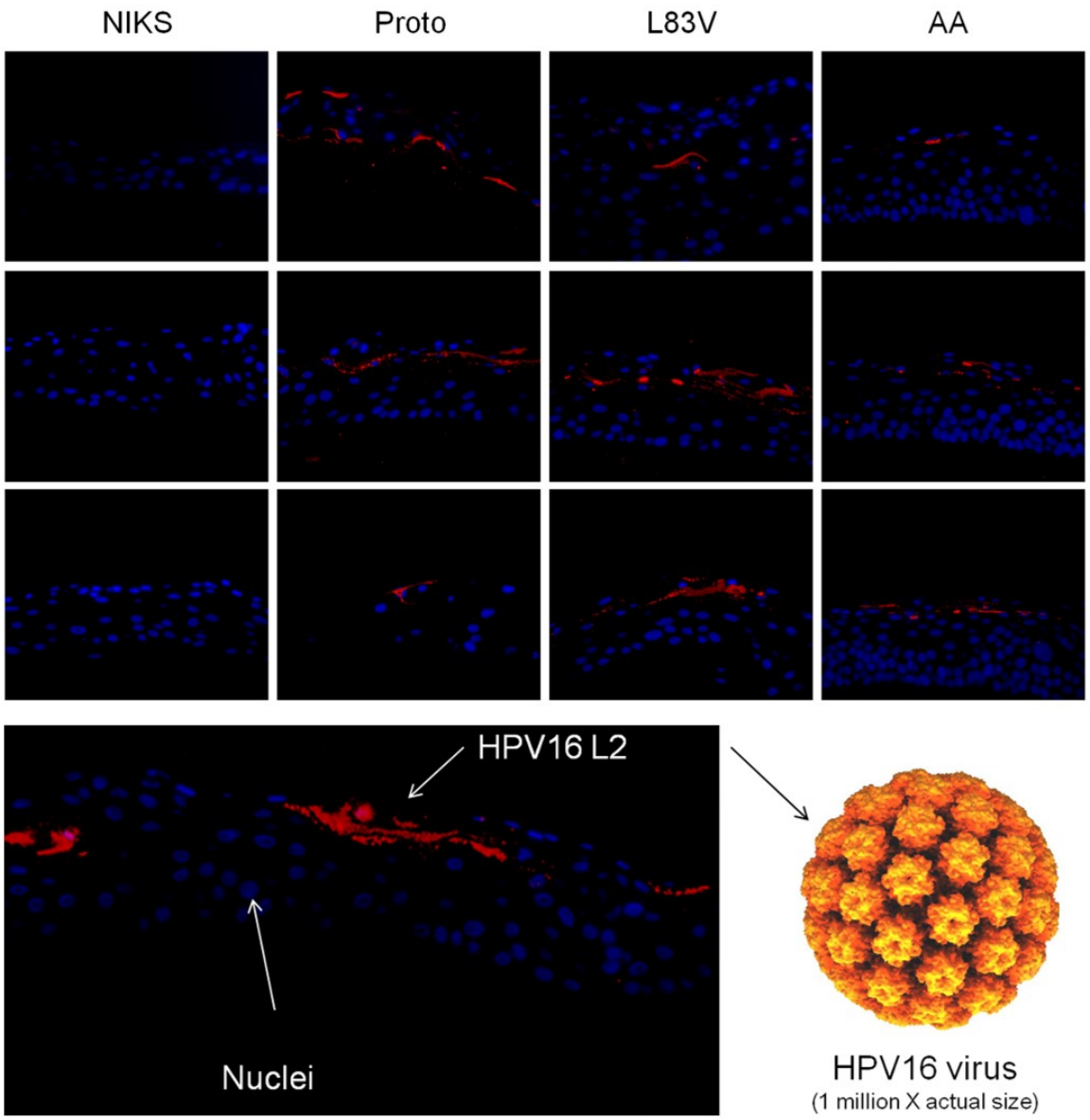

Figure 12. Active viral life cycle: HPV16 L2 capsid protein.

Fluorescent micrograph of sectioned formalin-fixed paraffin-embedded raft cultures (400X magnification, biological triplicates). Red fluorescence represents HPV16 L2 in the superficial zone of epithelium. Blue fluorescence represents nuclear-staining by DAPI. In rare cases (as in prototype #1), DAPI staining was inconsistent throughout the entire epithelium. Below, a labelled representative image is shown.

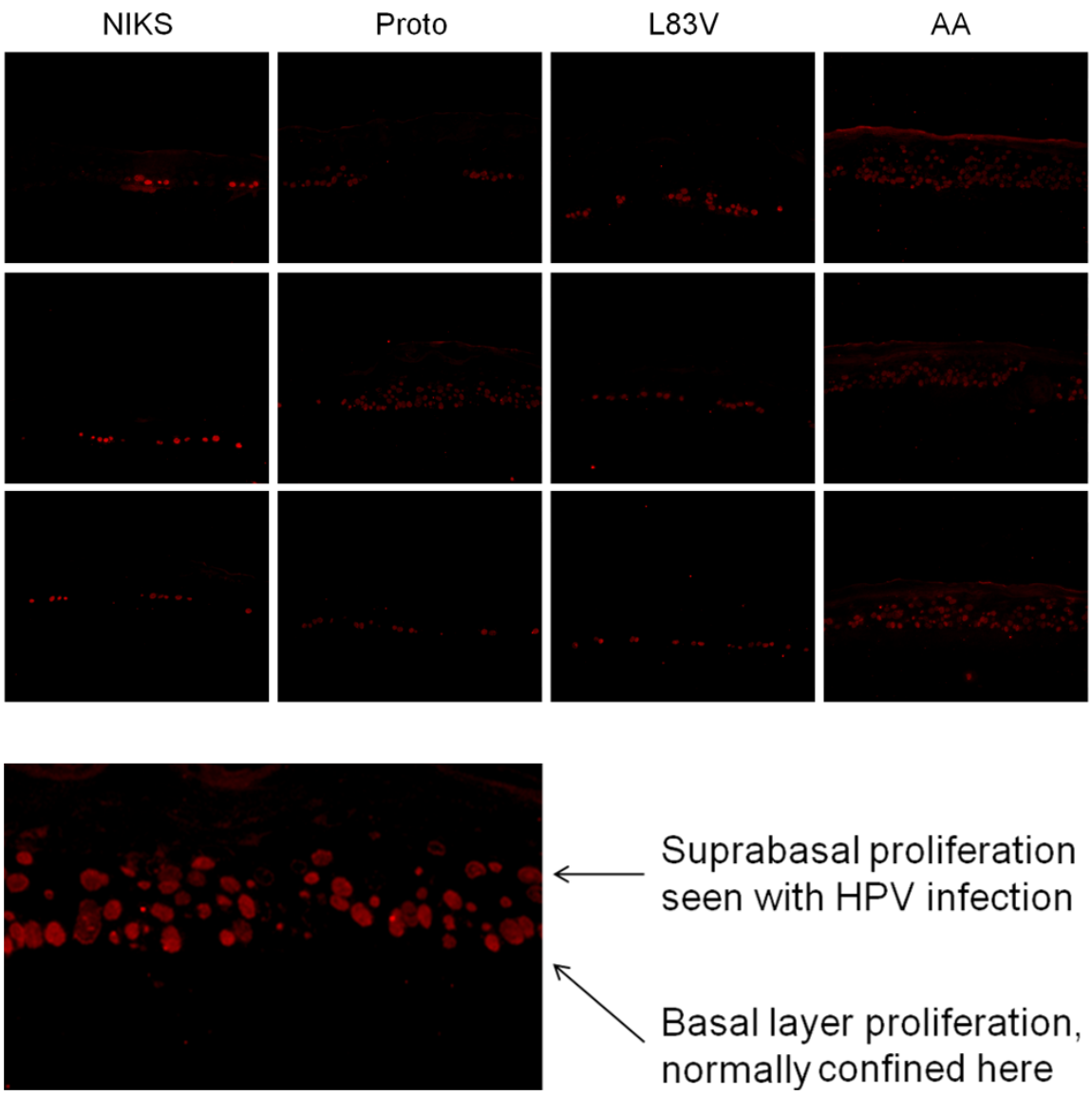

Figure 13. Proliferation marker BrdU.

Fluorescent micrograph of sectioned formalin-fixed paraffin-embedded raft cultures (200X magnification, biological triplicates). Red fluorescence represents proliferation marker BrdU, incorporated into nuclei of active cells. Minor background auto-fluorescence is apparent on section edges. Below, a labelled representative image is shown.

3.3.4 Differentation Pattern: K5 and K10 IHC

Keratin 5 was used as a basal cell differentiation marker while keratin 10 was used for suprabasal cell differentiation, based on previous reports (Zehbe et al., 2009). HPV16-containing rafts would likely have differential staining patterns: K5 suprabasal and K10 disrupted. In untransfected NIKS there was basal K5 staining with thick suprabasal K10 (**Figure 14**). In the variants, K5 staining was not isolated to the basal layer. In some areas of the variant epithelia K5 can be seen invading into the superficial zone and squamous layer. K10 is seen in the suprabasal and squamous layers for all rafts, but there are some areas of the variants where staining is disrupted and diminished.

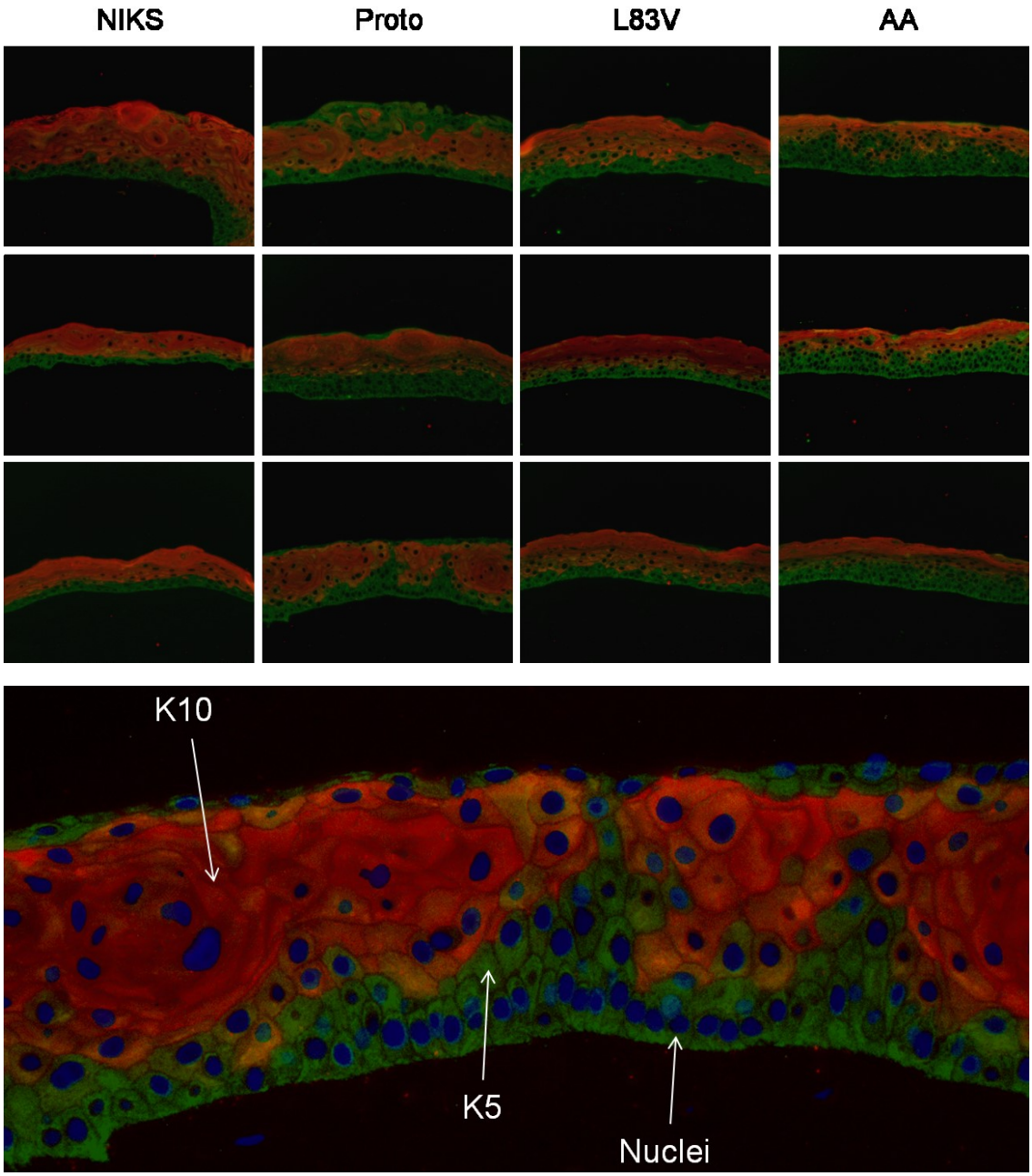

Figure 14. Differentiation markers K5/K10.

Fluorescent micrograph of sectioned formalin-fixed paraffin-embedded raft cultures (200X magnification, biological triplicates). Green fluorescence represents basal keratinocyte marker K5 while red represents suprabasal cell marker K10. Below, a labelled representative image is shown.

3.4 Viral Gene Expression Analysis by RT-qPCR

Viral mRNA transcript expression was measured from organotypic raft cultures grown for two weeks. Custom assays were designed and used in RT-qPCR reactions to relatively quantify the expression of HPV16 E6, E7, and E1^E4. E6 and E7 are the two prominent oncogenes while E1^E4 is suspected to be a marker of productive viral life cycle.

3.4.1 HPV16 E6

During a typical viral life cycle oncogene E6 expression is kept low by its modulator, E2 (Woodman et al., 2007). In our experiments, E6 expression was detected in all variants (Ct = 23 to 29) and not detected in the untransfected control (Ct = 40) (**Figure 15**). Relative expression of E6, in reference to stable HPRT1 expression, was not significantly different between variants ($P > 0.17$).

3.4.2 HPV16 E7

As with E6, oncogene E7 expression remains low during the viral life cycle (Woodman et al., 2007). In our experiments, E7 expression followed a similar pattern as E6, with no significant differences between variants (Ct = 20 to 26, $P > 0.17$) (**Figure 16**).

3.4.3 HPV16 E1^E4

The spliced transcript E1^E4 is used as a late viral life cycle marker (Bodily et al., 2011). In our experiments, E1^E4 was not detected in the untransfected control while expression was not significantly different between variants (Ct = 25 to 38, $P > 0.17$) (**Figure 17**). AA had extremely low but detectable E1^E4 expression (Ct ~38).

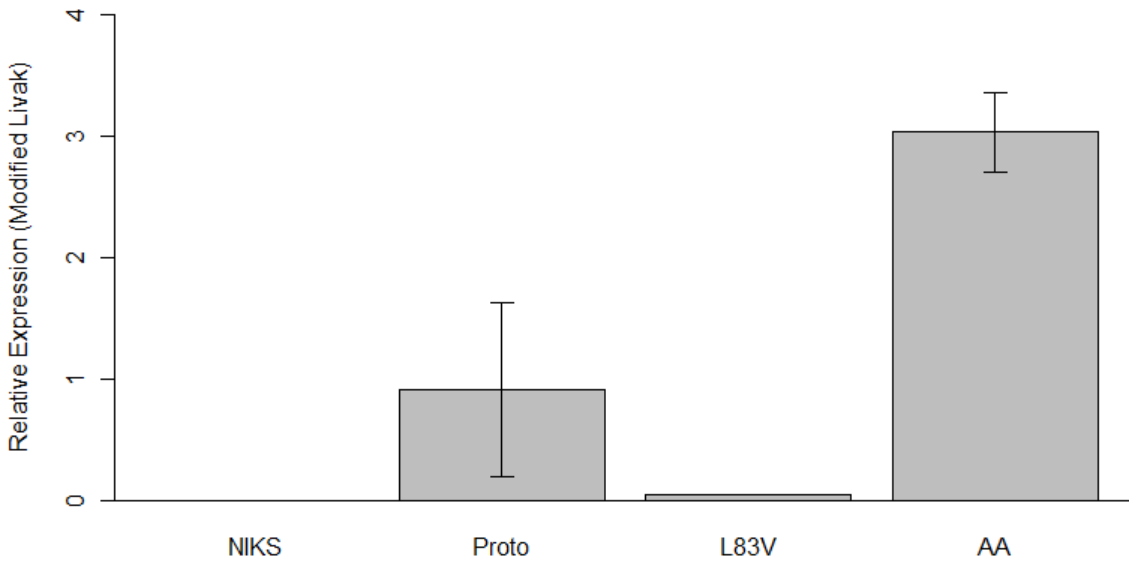

Figure 15. Relative expression of HPV16 E6 mRNA transcript.

Relative expression was calculated by the modified Livak method (2 ^ delta Ct) because the control/calibrator sample has zero viral gene expression. HPRT1 was used a reference gene. Although AA was significantly higher than NIKS ($P < 0.05$), E6 expression was not significantly different among variants ($P > 0.17$). Data are presented as mean +/- SEM ($n = 3$) while statistical analyses were performed by Krusk-Wallis rank sum test followed by Nemenyi post-hoc tests.

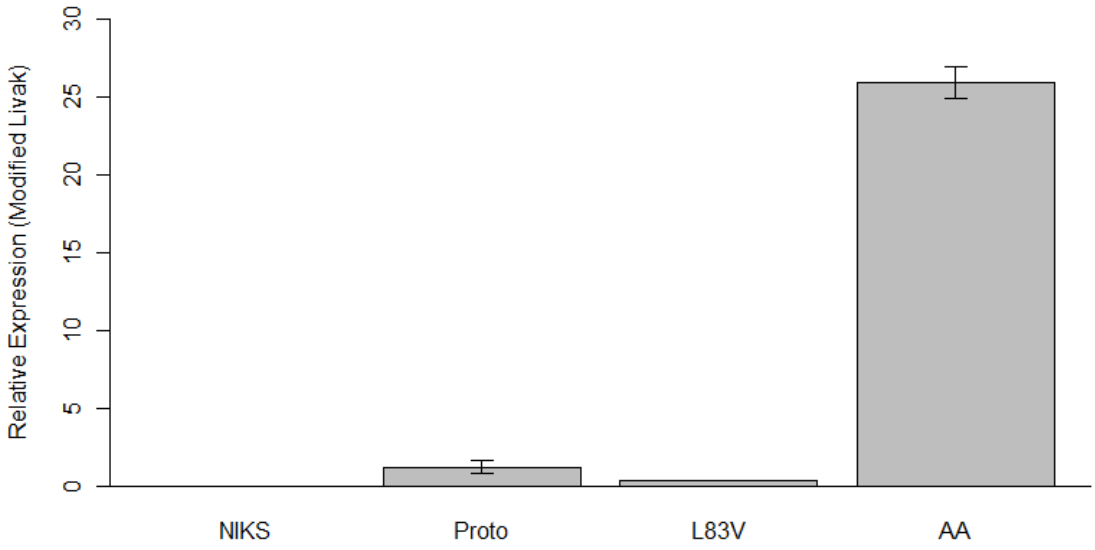

Figure 16. Relative expression of HPV16 E7 mRNA transcript.

Relative expression was calculated by the modified Livak method (2 ^ delta Ct) because the control/calibrator sample has zero viral gene expression. HPRT1 was used a reference gene. AA was significantly higher than NIKS ($P < 0.05$) while E7 expression was not significantly different among variants ($P > 0.17$). Data are presented as mean +/- SEM ($n = 3$) while statistical analyses were performed by Krusk-Wallis rank sum test followed by Nemenyi post-hoc tests.

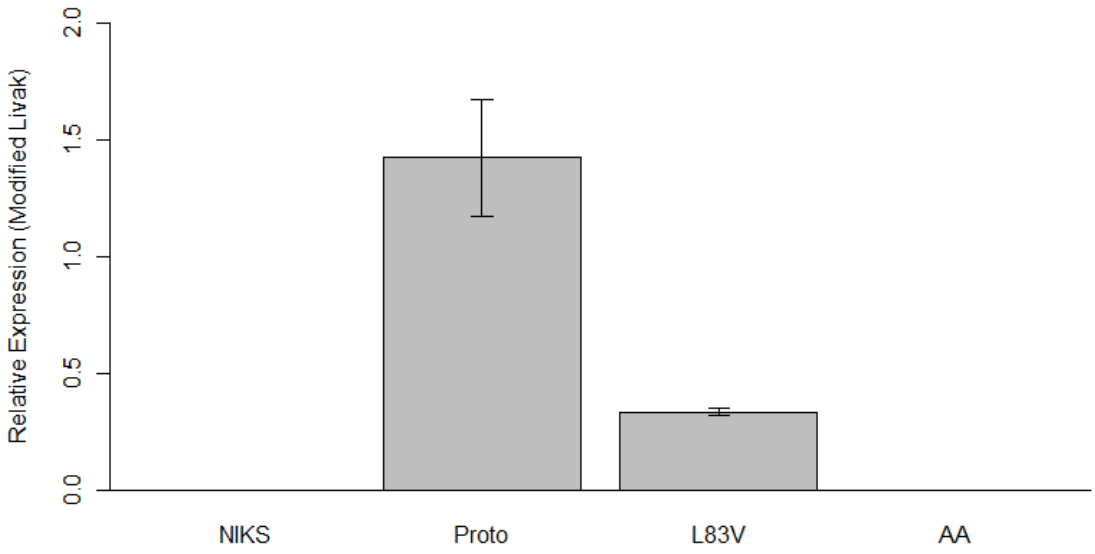

Figure 17. Relative expression of HPV16 E1^E4 mRNA transcript.

Relative expression was calculated by the modified Livak method (2 ^ delta Ct) because the control/calibrator sample has zero viral gene expression. HPRT1 was used a reference gene. Prototype was significantly higher than NIKS ($P < 0.05$) while E1^E4 expression was not significantly different among variants ($P > 0.17$). Although apparently zero, AA had low but detectable E1^E4 expression. Data are presented as mean +/- SEM ($n = 3$) while statistical analyses were performed by Krusk-Wallis rank sum test followed by Nemenyi post-hoc tests.

3.5 Innate Immune System Gene Expression Analysis by RT-qPCR

Variant-specific changes to interferon and TLR mRNA transcript expression were analyzed due to their importance in the host innate immune response.

3.5.1 Interferons

Interferon expression was low, evidenced by high Ct values. As a result, interpretations should be cautious. IFN beta had higher expression (Ct = 30 to 37), but with noticeable biological variability (but very low technical variability) in the HPV16+ variants (**Figure 18**). IFN gamma was undetected in all samples, but due to reference gene variation, L83V is significantly lower than NIKS ($P < 0.05$). IFN kappa had very low biological variability in all samples and higher detectable expression (Ct = 35 to 36). IFN kappa expression is significantly decreased in L83V (~0.57 fold change) and AA (~0.17 fold change) compared to NIKS and prototype ($P < 0.05$). Additionally, IFN kappa in AA is significantly lower than L83V ($P < 0.05$). IFN lambda was near the limit of detection (Ct ~ 40), with no significant differences found.

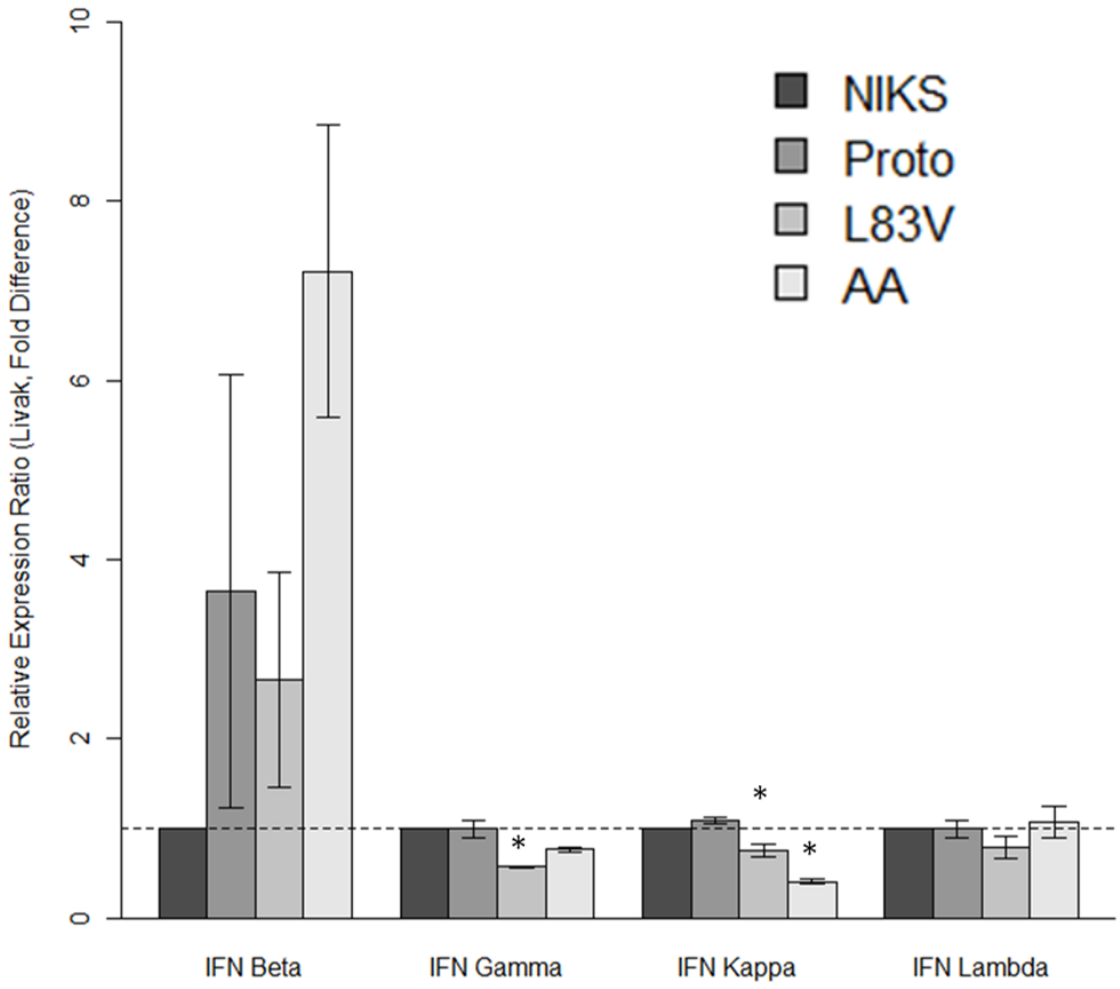

Figure 18. Relative expression ratio of interferons.

Fold difference, calculated by Livak method (2^delta delta Ct, NIKS as calibrator, HPRT1 as reference gene), square-root transformed to re-scale data. IFN beta expression is not significantly different ($P = 0.17$). IFN gamma expression is significantly lowered in L83V compared to NIKS and Proto ($P < 0.05$), but not AA ($P = 0.57$). L83V and AA have significantly down-regulated IFN kappa expression compared to NIKS and Proto ($P < 0.05$), while AA has significantly lower expression than L83V ($P < 0.05$). IFN lambda had no significant differences ($P = 0.47$). Data are means +/- SEM ($n = 3$): statistical analyses by ANOVA and TukeyHSD post-hoc. Asterisks represent significance.

3.5.2 Toll-Like Receptors

As seen with IFN expression analysis, TLR transcripts were also very low (**Figure 19**). TLR3 was the only assay that gave <35 Ct values (Ct = 28 to 30), while TLR4 and 9 have results between 35 and 40 Ct. TLR 7 and 8, however, are at the detection limit of 40 Ct and likely not valid for interpretation (any differences seen are mainly due to slight reference gene variation rather than actual transcript differences). Proto (~0.4 fold change), L83V (~0.2 fold change), and AA (~0.15 fold change) HPV16+ rafts all had significantly decreased TLR3 compared to untransfected NIKS ($P < 0.001$). Variant-specific TLR3 down-regulation was also observed, with L83V and AA having lower expression than Proto ($P < 0.05$). TLR4 expression was ~0.15 fold lower in L83V ($P < 0.05$) compared to NIKS. TLR7 expression was unchanged ($P > 0.05$). TLR8 expression was lower in L83V ($P < 0.05$), but likely invalid due to detection limit. TLR9 expression was ~2-3 fold higher in Proto and AA ($P < 0.05$) compared to NIKS.

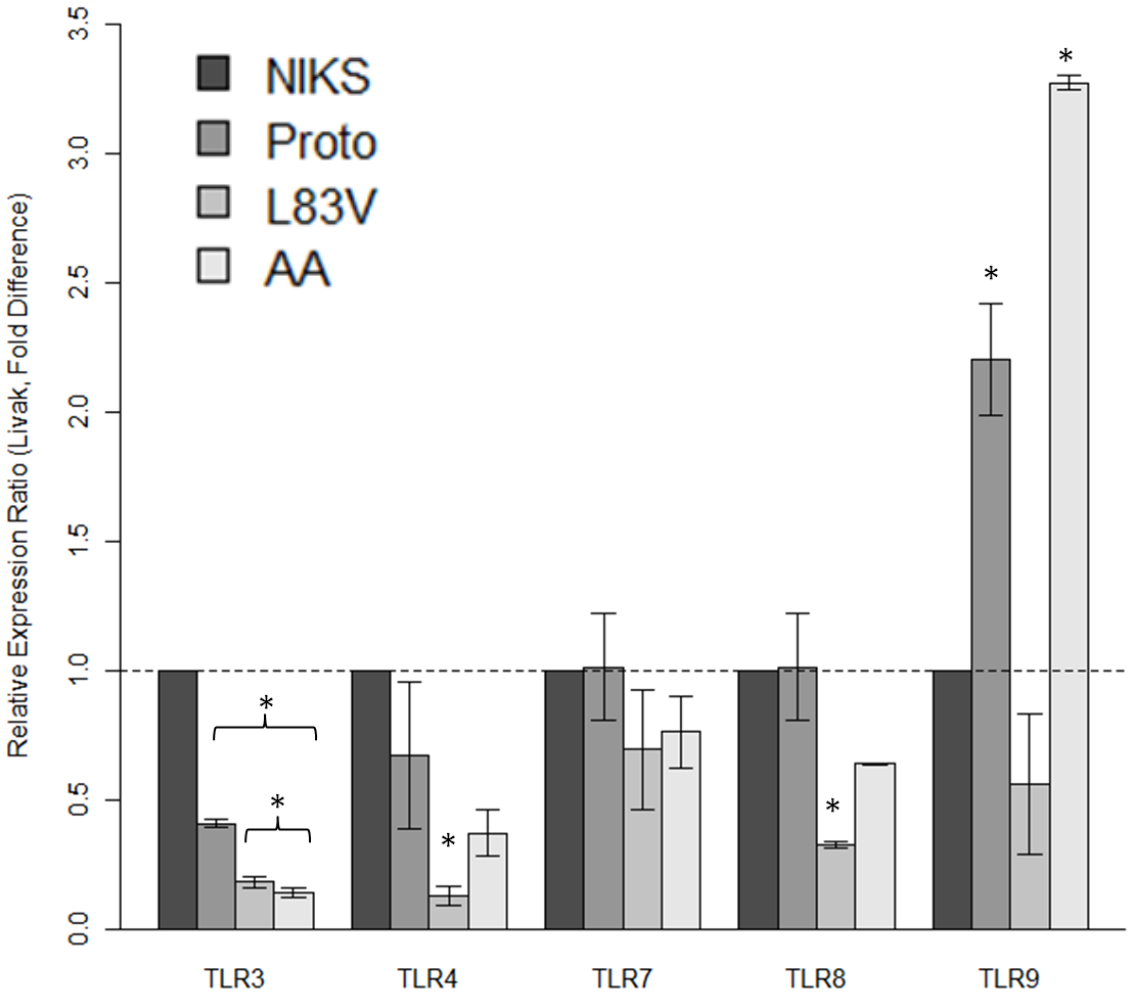

Figure 19. Relative expression ratio of toll-like receptors.

Fold difference, calculated by Livak method (2^delta delta Ct, NIKS as calibrator, HPRT1 as reference gene). TLR3 expression is lowered in Proto, AA, and L83V HPV16+ rafts ($P < 0.001$). AA and L83V TLR3 expression is less than Proto ($P < 0.05$). TLR4 expression is lower in L83V ($P < 0.05$). TLR7 expression was unchanged ($P > 0.05$). TLR8 expression was lower in L83V ($P < 0.05$). TLR9 expression was higher in Proto and AA ($P < 0.05$). Data are presented as mean +/- SEM ($n = 3$): statistical analyses by ANOVA and TukeyHSD post-hoc tests. Asterisks represent significance.

4 DISCUSSION

4.1 Establishment of HPV16 E6 Variant Cell Lines

The first step was to prepare the experimental groups using various molecular biology techniques such as transformation, restriction digest, ligation, and transfections. NIKS were chosen as host cells rather than primary human foreskin keratinocytes because of their ability to be grown indefinitely and undergo normal differentiation (Flores et al., 1999; Allen-Hoffman et al., 2000). NIKS transfected with full-length HPV16 E6 variant DNA were successfully obtained and verified via E6 DNA PCR (**Figure 9**). As discussed by Lambert et al. (2005), transfectants with episomal DNA required special care to prevent genomic integration of viral DNA. Additionally, all transfectants were prepared in the same way, limiting any differences due to technical variability between experiments. Another important factor to successful establishment of transfectants was ensuring *Mycoplasma* contamination was not present. *Mycoplasma* are a common cell-culture contaminant and cause low transfection efficiencies (Xia et al., 1997) along with gene expression changes (Jung et al., 2003) in host cultures. Given the purpose of this study was to introduce viral DNA via transfection followed by gene expression analyses, a *Mycoplasma* infection would have been detrimental to validity. Routine testing for contamination was performed, allowing us to be confident that expression changes in our cultures were due to experimental conditions rather than an infection.

4.2 Development of Organotypic Model

Once HPV16 E6 variant cell lines were established it was necessary to employ an organotypic tissue culture model to enable an active viral life cycle (Lambert et al., 2005). To accurately reproduce the skin, it's necessary to recreate the important layers: dermis and epidermis (Lambert et al., 2005). For recreating the dermis, collagen was embedded with fibroblasts and formed into solidified plugs. This structure provides a life-like structural support for keratinocytes to grow upon. Through many trials, it was determined that rat tail collagen, type I, at a concentration between 3.75 and 4.00 mg/mL, was ideal (**Figure 11**). Bovine collagen and lower concentrations (such as 2.00 mg/mL) were unsuccessful, yielding weak dermal equivalents. Early-passage human foreskin fibroblasts yielded the best epidermal growth. Given that non-immortal primary cultures senesce after fixed population doublings (Hayflick, 1965), it's reasonable to suggest that high-passage fibroblasts can result in poor raft growth. When creating the basal keratinocyte layer atop the dermis, it's essential to use media containing epidermal growth factor (EGF). EGF binds to EGF-receptor leading to activation of DNA transcription; proliferation of NIKS cells is severely inhibited by its absence and formation of a fully-packed basal layer is retarded (Allen-Hoffman et al., 2000). After the basal keratinocyte layer is established, differentiation can be induced by lifting the raft onto a membrane, forming an air-liquid interface (Poumay and Coquette, 2007). If not done carefully, lifting can disrupt or destroy raft cultures. Additionally, differentiation of NIKS requires media with the omission of EGF and supplementation with calcium (Lambert et al., 2005), fed through the bottom of each membrane in a 6 well-plate.

4.3 Phenotypic Characterization of Rafts

As verified by morphological assessment, raft cultures were successfully grown to mimic human skin (**Figure 11**). However, a common finding in all raft cultures was different epithelial thickness across the diameter of each circular raft. The outer edges of each raft were thicker than the middle, indicating uneven distribution of cells during establishment or a lack of nutrient medium being fed into the centre. Given that the rafts were atop a membrane in a 6-well plate, it was easy to ensure the entire bottom of the raft was interfaced with medium. When keratinocytes were added they were confirmed via microscopy to be homogenously distributed. The likely culprit is collagen contraction within 24-well plates after seeding keratinocytes, causing the cells to be distally clumped (Lambert at al., 2005). Although the lack of a full-thickness epithelium throughout an entire raft is disconcerting from a morphological perspective, it doesn't preclude verification of an active viral life cycle (the ultimate test). However, to determine if a better raft model was possible an alternative approach was attempted (**Appendix 7.1**).

An inferential study on innate immune evasion in an early-infection scenario requires the confirmation of an active viral life cycle: one that is capable of manipulating keratinocyte differentiation and producing virus. The best direct evidence for this would be visual confirmation of viral particles using a transmission electron microscope. Unfortunately, this method requires an ultramicrotome to cut extremely thin tissue sections, a service not available to me. Viral life cycle was instead confirmed using standardized immunohistochemistry for a set of specific markers: HPV16 L2 indicating

end-stage production of virus, BrdU incorporation for cell proliferation (Flores et al., 1999), and keratins 5 and 10 for differentiation pattern (Zehbe et al., 2009).

Presence of HPV16 minor capsid protein L2 in the upper layers of epithelium, as supported by previous literature, is strong evidence of an active viral life cycle (Doorbar, 2005). L2 along with L1 are produced during late-stage expression to encapsidate the supply of viral genomes before complete particles are released into the environment. Interestingly, the AA variant having the lowest detectable L2 (**Figure 12**) indicates that AA may have a temporally longer or shorter viral life cycle, along with reduced productive output. Suprabasal incorporation of BrdU into DNA indicates basal keratinocytes that are continuing to proliferate rather than terminally differentiating. HPV16 variants increased suprabasal incorporation compared to NIKS (**Figure 13**), indicating an active effect of early gene expression by E6 and E7 (Flores et al., 1999). Another interesting finding is that nearly every suprabasal cell of AA is actively undergoing DNA synthesis. Taken with the observation that L2 staining is minimal, this points toward a longer viral life cycle in AA. Additionally, keratin dysregulation in AA reveals that basal keratinocyte marker K5 is present in the suprabasal proliferating cells (**Figure 14**). Most evident in prototype, there are disruptions to differentiation marker K10, indicating a mixing of regular cell compartments. Although to a greater extent, similar differentiation patterns caused by HPV16 E6 variants have been observed in retrovirally transduced NIKS (Zehbe et al., 2009). Overall, phenotypic characterization of the organotypic cultures reveals that this was an appropriate model for study.

4.4 Viral Gene Expression

With HPV16 E6 variant-transduced keratinocytes successfully grown using a verified model system, the next logical step was molecular analyses. Changes in messenger RNA (mRNA) expression are a useful measure of the molecular environment within cells (Crick, 1970). Although mRNA transcript expression detected using RT-qPCR may not unerringly equate to the amount of that protein, it's a valuable method to quantify activation of genes. The primary disadvantage of standard RT-qPCR without pre-amplification is the difficulty of detecting low-copy number transcripts due to detection limits (DeCarlo et al., 2010). The reliability of data (cycle thresholds) diminishes as the detection limit is approached (Ct = 40). A threshold is typically set as an arbitrary cut-off for reliable data (Bustin et al., 2009). Finally, the analysis of Ct values typically requires normalization to a reference gene and control sample; for this study, relative expression was calculated based on the Livak method, since Ct values are exponential in nature (Livak and Schmittgen, 2001).

To understand the state of viral gene expression, early oncogenes E6 and E7 were measured, as well as viral life cycle marker E1^E4. Variant-specific expression differences were not found, likely due to a lack of statistical power (**Figures 15, 16, 17**). Sample variances were heterogeneous and not amenable to more powerful parametric analysis. Additionally, the small sample size coupled with small effect size do not allow detectable differences to be found. Although not significant, an increase in E6 and E7 expression in AA indicates early expression differences, and a likely delay of the viral life cycle. This fits with the low detection of E1^E4 (**Figure 17**), which is expressed

during the productive stage of the viral life cycle (Bodily et al., 2011). Protein-level detection by western blot or immunohistochemistry can be used in the future to discern if there are actually any differences between variants.

4.5 Innate Immune System Gene Expression

As hypothesized, we found variant-specific differences in the host keratinocyte innate immune system activation and response. As described in the previous section, transcripts at low level pose a problem for analysis and interpretation. Innate immune system genes, such as some interferons and toll-like receptors, are known to be expressed at low levels (DeCarlo et al., 2010; DeCarlo et al., 2012). With the exception of IFN-κ and TLR3, most innate immunity genes analyzed are near the detection limit (Ct = 35 to 40, possibly not reliable, and do not offer valid interpretation (**Figures 18, 19**). Further experiments with a pre-amplification step, as described by DeCarlo et al., 2010, are required to raise the relative transcript-levels to a reliably detectable range.

IFNs and TLRs are typically activated by viral infection; dengue virus replication elicits an antiviral innate immune response in infected human keratinocytes (Surasombatpattana et al., 2011). Specifically, TLR3 is cyclically expressed as a trans-endosomal membrane receptor that responds to dsRNA, a product of most viral life cycles (Jorgenson et al., 2005). TLR3, which can be induced by IFN expression, leads to immune response factor activation, causing transcription of TNF, COX2, and IL-18 (Khoo et al., 2011). In response to most viral infections, the typical response is an activation of IFNs and TLR3. However, our results suggest that an active HPV16 viral life cycle, specifically of the L83V and AA variant, evades the host innate immune

response by down-regulating IFN-κ and TLR3 (**Figures 18, 19**). As reported by Reiser at al. (2011), high-risk HPVs, such as type 16, repress constitutive IFN-κ transcription via E6, preventing induction of pathogen recognition receptors such as TLR3 and other antiviral genes. Studies of mucosal swab samples build upon this evidence, showing that in cases of persistent infections TLR3 expression was dampened (Daud et al., 2011). Recent studies of IFN, TLR, and integrin expression using *ex vivo* samples has revealed the unique immune responses in the microenvironment of normal, dysplastic, and carcinoma tissues (DeCarlo et al., 2008; DeCarlo et al., 2010; DeCarlo et al., 2011; Werner et al., 2012). The results reported here fill an important void, in that we have now characterized the effects of an early-infection on innate immunity in the context of the variants. Our results, taken together with the epidemiological evidence of variant-specific prevalences in cervical cancer (Zehbe et al., 1998), and the growing evidence offered by transformation studies (Niccoli et al., 2012), suggest that immune evasion by AA and L83V may lead to a state of persistent infection, with increased transformation potential, and higher prevalence in invasive cervical cancer.

5 CONCLUSIONS AND FUTURE DIRECTIONS

Overall, an organotypic tissue culture model for HPV-infected skin was successfully established. Phenotypic characterization verified the experimental model, while molecular analyses yielded evidence for significant variant-specific decrease of antiviral innate immune responses in host keratinocytes. Asian-American and L83V HPV16 E6 variants appear to have increased host immune evasion capabilities over the

Prototype. Interestingly, productive viral life cycle was lowest in the AA variant: an unexpected result. Further experimentation is required to determine if there are temporal differences between the viral life cycles of the variants. Additionally, pre-amplification is required to reliably detect low-level transcripts. These future experiments will determine if the differential gene expression patterns are reproducible and if the viral life cycle occurs earlier or later in AA. A delayed viral life cycle in AA could have implications for its immune evasion capabilities.

Since these experiments yield variant-specific effects within the host transcriptome a future direction is to employ high-throughput analysis such as Affymetrix microarray or RNA-sequencing followed by bioinformatics analyses. Such a study will yield a global transcript expression profile. HPV16 E6 variant profiles can be compared to HPV-negative NIKS profiles to construct an infectome map of all host gene expression changes in response to an active viral life cycle. In addition to bioinformatics analyses, protein-level detection of E6 can be used to monitor functional effects on host proteins (Jackson and Zehbe, 2012). Finally, the major limitation of the organotypic tissue culture model is the lack of a circulatory and an adaptive immune system. These *in vitro* limitations could be ameliorated by using an appropriate *in vivo* mouse model.

6 REFERENCES

Allen-Hoffmann, B.L., Schlosser, S.J., Ivarie, C.A., Sattler, C.A., Meisner, L.F., O'Connor, S.L., 2000. Normal growth and differentiation in a spontaneously immortalized near-diploid human keratinocyte cell line, NIKS. J Invest Dermatol 114, 444-455.

Auersperg, N., 1964. Long-term cultivation of hypodiploid human tumor cells. J Natl Cancer Inst 32, 135-163.

Bodily, J.M., Mehta, K.P.M., Cruz, L., Meyers, C., Laimins, L.A., 2011. The E7 open reading frame acts in cis and in trans to mediate differentiation-dependent activities in the human papillomavirus type 16 life cycle. J Virol 85, 8852-8862.

Boehme, K.W., Compton, T., 2004. Innate sensing of viruses by toll-like receptors. J Virol 78, 7867-7873.

Box, G.E.P., 1976. Science and statistics. J Am Stat Assoc, 791-799.

Box, G.E.P., Jenkins, G.M., Reinsel, G.C., 1976. Time series analysis. Holden-day San Francisco.

Bustin, S.A., Benes, V., Garson, J.A., Hellemans, J., Huggett, J., Kubista, M., Mueller, R., Nolan, T., Pfaffl, M.W., Shipley, G.L., 2009. The MIQE guidelines: minimum information for publication of quantitative real-time PCR experiments. Clin Chem 55, 611-622.

Chen, TR., 1977 In situ detection of Mycoplasma contamination in cell cultures by fluorescent Hoechst 33258 stain. Exp Cell Res 104, 255.

Crick, F., 1970. Central dogma of molecular biology. Nature 227, 561-563.

Daud, I.I., Scott, M.E., Ma, Y., Shiboski, S., Farhat, S., Moscicki, A.B., 2011. Association between toll-like receptor expression and human papillomavirus type 16 persistence. Int J Cancer 128, 879-886.

Dayyani, F., Etzel, C.J., Liu, M., Ho, C.H., Lippman, S.M., Tsao, A.S., 2010. Meta-analysis of the impact of human papillomavirus (HPV) on cancer risk and overall survival in head and neck squamous cell carcinomas (HNSCC). Head Neck Oncol 2, 15.

DeCarlo, C.A., Escott, N.G., Werner, J., Robinson, K., Lambert, P.F., Law, R.D., Zehbe, I., 2008. Gene expression analysis of interferon κ in laser capture microdissected cervical epithelium. Anal Biochem 381, 59-66.

DeCarlo, C.A., Severini, A., Edler, L., Escott, N.G., Lambert, P.F., Ulanova, M., Zehbe, I., 2010. IFN-κ, a novel type I IFN, is undetectable in HPV-positive human cervical keratinocytes. Lab Invest 90, 1482-1491.

DeCarlo, C.A., Rosa, B., Jackson, R., Niccoli, S., Escott, N.G., Zehbe, I., 2012. Toll-Like Receptor Transcriptome in the HPV-Positive Cervical Cancer Microenvironment. Clin Dev Immunol 2012, 785825.

Doorbar, J., 2005. The papillomavirus life cycle. Journal of clinical virology 32, 7-15.

Fleckenstein, E., Drexler, H.G., 1996. Elimination of Mycoplasma contamination in cell cultures. Biochemica 1, 48-51.

Flores, E.R., Allen-Hoffmann, B.L., Lee, D., Sattler, C.A., Lambert, P.F., 1999. Establishment of the human papillomavirus type 16 (HPV-16) life cycle in an immortalized human foreskin keratinocyte cell line. Virology 262, 344-354.

Flores, E.R., Allen-Hoffmann, B.L., Lee, D., and Lambert, P.F., 2000. The human papillomavirus type 16 E7 oncogene is required for the productive stage of the viral life cycle. J Virol 74, 6622–6631.

Friedl, F., Kimura, I., Osato, T., Ito, Y., 1970. Studies on a new human cell line (SiHa) derived from carcinoma of uterus. I. Its establishment and morphology. Proc Soc Exp Biol Med 135, 543-545.

Genther, S.M., Sterling, S., Duensing, S., Münger, K., Sattler, C., and Lambert, P.F., 2003. Quantitative role of the human papillomavirus type 16 E5 gene during the productive stage of the viral life cycle. J Virol 77, 2832–2842.

Hamid, N.A., Brown, C., Gaston, K., 2009. The regulation of cell proliferation by the papillomavirus early proteins. Cell Mol Life Sci 66, 1700-1717.

Hayflick, L., 1965. The limited in vitro lifetime of human diploid cell strains. Exp Cell Res 37, 614-636.

Jackson, R., Zehbe, I., 2012. Quantitative immunocytochemical detection of the human papillomavirus type 16 E6 oncoprotein. Virology (manuscript submitted).

Jorgenson, R.L., Young, S.L., Lesmeister, M.J., Lyddon, T.D., Misfeldt, M.L., 2005. Human endometrial epithelial cells cyclically express Toll-like receptor 3 (TLR3) and exhibit TLR3-dependent responses to dsRNA. Hum Immunol 66, 469-482.

Jung, H, Wang, S.Y., Yang, I.W., Hsueh, D.W., Yang, W.J., Wang, T.H., Wang, H.S., 2003. Detection and treatment of mycoplasma contamination in cultured cells. Chang Gung Med J 26, 250-258.

Kessis, T.D., Slebos, R.J., Nelson, W.G., Kastan, M.B., Plunkett, B.S., Han, S.M., Lorincz, A.T., Hedrick, L., Cho, K.R., 1993. Human papillomavirus 16 E6

expression disrupts the p53-mediated cellular response to DNA damage. Proc Natl Acad Sci USA 90, 3988-3992.

Khoo, J.J., Forster, S., Mansell, A., 2011. Toll-like receptors as interferon-regulated genes and their role in disease. J Interferon Cytokine Res 31, 13-25.

Kumar, A., Zhao, Y., Meng, G., Zeng, M., Srinivasan, S., Delmolino, L.M., Gao, Q., Dimri, G., Weber, G.F., Wazer, D.E., Band, H., Band, V., 2002. Human papillomavirus oncoprotein E6 inactivates the transcriptional coactivator human ADA3. Mol Cell Biol 22, 5801-5812.

Lagrange, M., Charbonnier, S., Orfanoudakis, G., Robinson, P., Zanier, K., Masson, M., Lutz, Y., Trave, G., Weiss, E., Deryckere, F., 2005. Binding of human papillomavirus 16 E6 to p53 and E6AP is impaired by monoclonal antibodies directed against the second zinc-binding domain of E6. J Gen Virol 86, 1001-1007.

Lambert, P.F., Ozbun, M.A., Collins, A., Holmgren, S., Lee, D., and Nakahara, T., 2005. Using an immortalized cell line to study the HPV life cycle in organotypic “raft” cultures. Methods Mol Med 119, 141–155.

Lechner, M.S., Mack, D.H., Finicle, A.B., Crook, T., Vousden, K.H., Laimins, L.A., 1992. Human papillomavirus E6 proteins bind p53 in vivo and abrogate p53-mediated repression of transcription. EMBO J 11, 3045-3052.

Livak, K.J., Schmittgen, T.D., 2001. Analysis of relative gene expression data using real-time quantitative PCR and the 2-[Delta][Delta] CT method. Methods 25, 402-408.

Mantovani, F., Banks, L., 2001. The human papillomavirus E6 protein and its contribution to malignant progression. Oncogene 20, 7874-7887.

McCance, D.J., Kopan, R., Fuchs, E., and Laimins, L.A., 1988. Human papillomavirus type 16 alters human epithelial cell differentiation in vitro. Proc Natl Acad Sci 85, 7169-7173.

Meyers, C., Bromberg-White, J.L., Zhang, J., Kaupas, M.E., Bryan, J.T., Lowe, R.S., and Jansen, K.U., 2002. Infectious virions produced from a human papillomavirus type 18/16 genomic DNA chimera. J Virol 76, 4723-4733.

Miller, S.A., Harley, J.P., 2002. Zoology. McGraw-Hill.

Navratil, V., De Chassey, B., Combe, C.R., Lotteau, V., 2011. When the human viral infectome and diseasome networks collide: towards a systems biology platform for the aetiology of human diseases. BMC Syst Biol 5, 13.

Niccoli, S., Abraham, S., Zehbe, I., 2012. The carcinogenic properties of naturally occurring human papillomavirus 16 E6 oncogene variants. J Virol (accepted).

Nunc Nalgene, 1998. Cryopreservation Manual.

O'Brien, P.M., Saveria Campo, M., 2003. Papillomaviruses: a correlation between immune evasion and oncogenicity? Trends Microbiol 11, 300-305.

Pattillo, R.A., Hussa, R.O., Story, M.T., Ruckert, A.C., Shalaby, M.R., Mattingly, R.F., 1977. Tumor antigen and human chorionic gonadotropin in CaSki cells: a new epidermoid cervical cancer cell line. Science 196, 1456-1458.

Poumay, Y., Coquette, A., 2007. Modelling the human epidermis in vitro: tools for basic and applied research. Arch Dermatol Res 298, 361-369.

R Development Core Team. 2008. R: A language and environment for statistical computing. R Foundation for Statistical Computing, Vienna, Austria. ISBN 3-900051-07-0, URL http://www.R-project.org.

Richard, C., Lanner, C., Naryzhny, S., Sherman, L., Lee, H., Lambert, P., Zehbe, I., 2010. The immortalizing and transforming ability of two common human papillomavirus 16 E6 variants with different prevalences in cervical cancer. Oncogene 29, 3435-3445.

Reiser, J., Hurst, J., Voges, M., Krauss, P., Münch, P., Iftner, T., Stubenrauch, F., 2011. high-risk human papillomaviruses repress constitutive kappa interferon transcription via E6 to prevent pathogen recognition receptor and antiviral-gene expression. J Virol 85, 11372-11380.

Russell, W.C., Newman, C., Williamson, D.H., 1975. A simple cytochemical technique for demonstration of DNA in cells infected with mycoplasmas and viruses. Nature 253, 461-462.

Schimke, R.T., Berlin, C.M., Sweeney, E.W., Carroll, W.R., 1966. The generation of energy by the arginine dihydrolase pathway in Mycoplasma hominis 07. J Biol Chem 241, 2228-2236.

Scheffner, M., Takahashi, T., Huibregtse, J.M., Minna, J.D., Howley, P.M., 1992. Interaction of the human papillomavirus type 16 E6 oncoprotein with wild-type and mutant human p53 proteins. J Virol 66, 5100-5105.

Schneider, C.A., Rasband, W.S., Eliceiri, K.W., 2012. "NIH Image to ImageJ: 25 years of image analysis". Nature Methods 9, 671-675.

Stanley, M.A., Pett, M.R., Coleman, N., 2007. HPV: from infection to cancer. Biochem Soc Trans 35, 1456-1460.

Stoppler, M.C., Ching, K., Stoppler, H., Clancy, K., Schlegel, R., Icenogle, J., 1996. Natural variants of the human papillomavirus type 16 E6 protein differ in their

abilities to alter keratinocyte differentiation and to induce p53 degradation. J Virol 70, 6987–6993.

Surasombatpattana, P., Hamel, R., Patramool, S., Luplertlop, N., Thomas, F., Desprès, P., Briant, L., Yssel, H., Missé, D., 2011. Dengue virus replication in infected human keratinocytes leads to activation of antiviral innate immune responses. Infect Genet Evol 11, 1664-1673.

Werner, J., DeCarlo, C.A., Escott, N., Zehbe, I., Ulanova, M., 2012. Expression of integrins and Toll-like receptors in cervical cancer: Effect of infectious agents. Innate Immunity 18, 55-69.

Wilson, B.A., Salyers, A.A., Whitt, D.D., Winkler, M.E., 2011. Bacterial pathogenesis: a molecular approach. American Society for Microbiology (ASM).

Woodman, C.B.J., Collins, S.I., Young, L.S., 2007. The natural history of cervical HPV infection: unresolved issues. Nature Reviews Cancer 7, 11-22.

Xia, H., Fitzgerald, J., Bredt, D.S., Forsayeth, J.R., 1997. Detection of mycoplasma infection of mammalian cells. Biotechniques 22, 934-936.

Yasumoto, S., Burckhardt, A.L., Doniger, J., and DiPaolo, J.A., 1986. Human papillomavirus type 16 DNA-induced malignant transformation of NIH 3T3 cells. J Virol 57, 572-577.

Zehbe, I., Wilander, E., Delius, H., Tommasino, M., 1998. Human papillomavirus 16 E6 variants are more prevalent in invasive cervical carcinoma than the prototype. Cancer Res 58, 829-833.

Zehbe, I., Richard, C., DeCarlo, C.A., Shai, A., Lambert, P.F., Lichtig, H., Tommasino, M., Sherman, L., 2009. Human papillomavirus 16 E6 variants differ in their

dysregulation of human keratinocyte differentiation and apoptosis. Virology 383, 69-77.

zur Hausen, H., 1996. Papillomavirus infections--a major cause of human cancers. Biochim Biophys Acta 1288, 55-78.

zur Hausen, H., 2002. Papillomaviruses and cancer: from basic studies to clinical application. Nat Rev Cancer 2, 342-350.

Zur Hausen, H., 2007. Infections causing human cancer. Wiley-VCH, Germany.

7 APPENDIX

7.1 Alternative Organotypic Culture Model

As an additional validation of the organotypic model culture, an alternative culture system was morphologically assessed. Given that the main drawback of our default culturing system was variable epithelial thickness and differentiation between distal and medial areas, the use of a scaffold was justified. Alvetex® 6-well polystyrene scaffold inserts (Reinnervate, Cat. No. AVP004-3) were prepared and grown with NIKS cells according to supplier protocols employing collagen coating. Routine culturing of Alvetex® scaffolds was troublesome due to the increased volume of media required and porosity of the membrane. The scaffolds are raised and require 5x more medium than other rafts. Additionally, collagen and cells seeded on top of the scaffold leaked through the membrane, contaminating the 6-well plates. Plates had to be changed frequently to prevent media sequestering by these cells. Finally, the membrane needs to be cut from the plastic supports, increasing the amount of manipulation while harvesting. Morphological assessment of NIKS grown on an Alvetex® scaffold show poor epithelial differentiation across the entire layer and a disrupted dermis (**Figure 20**). Fibroblasts and collagen appear to have leaked through and settled to the bottom of the scaffold.

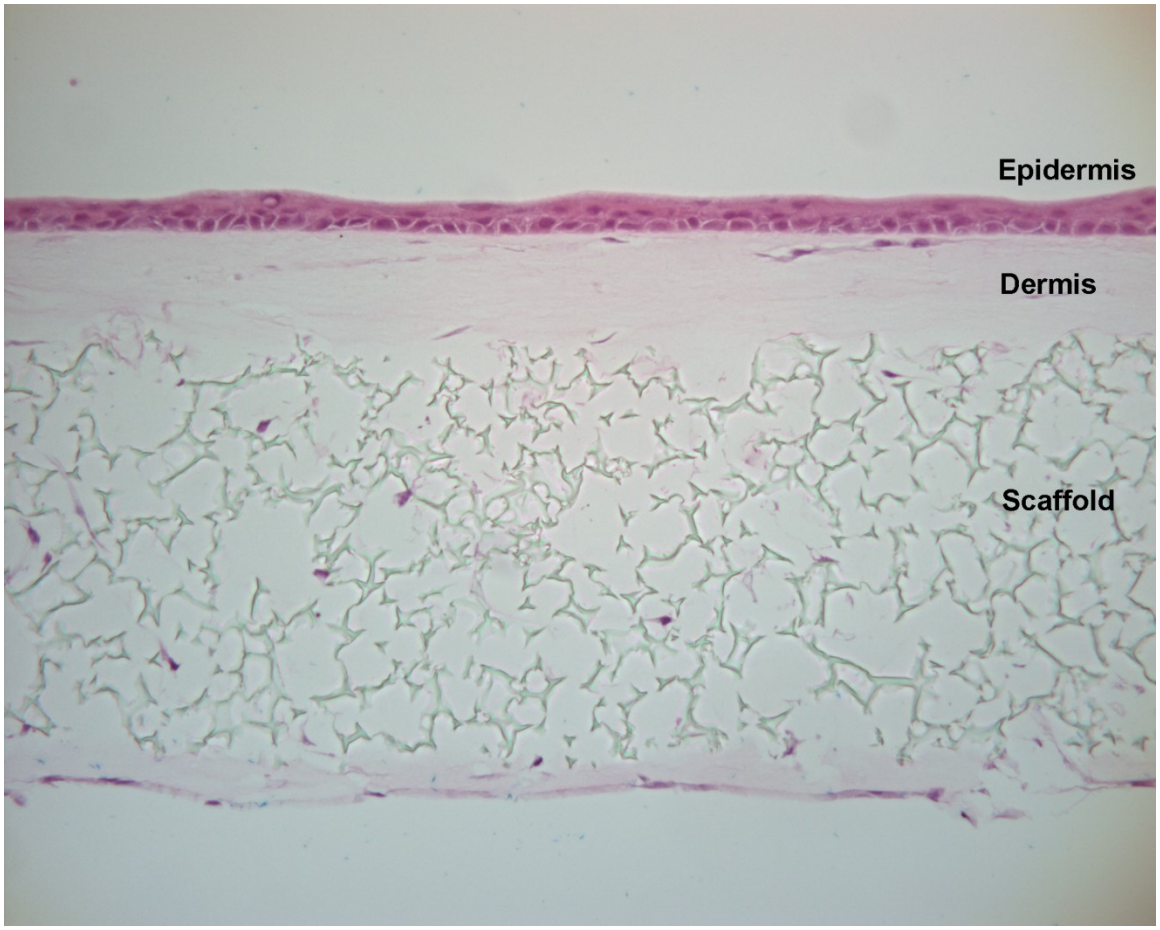

Figure 20. NIKS culture morphology with Alvetex® scaffold.

Haematoxylin and eosin stain (200X magnification) of cross-sectioned formalin-fixed paraffin-embedded NIKS organotypic culture grown for 2 weeks using an Alvetex® scaffold. The epidermis, dermis, and scaffold layers are labelled.

Overall, our organotypic culture model performed better than Alvetex® scaffolds in terms of simplicity, cost effectiveness, and morphology. However, using a classical culture format with a dermal equivalent (collagen with embedded fibroblasts) does not seem appropriate for these scaffolds. Rather than mimicking the dermis atop, it may be possible to grow fibroblasts directly within the scaffold without an exogenous collagen matrix.